STUDIES OF ATOMIC AND MOLECULAR PROCESSES AND PROPERTIES IN THE RANDOM PHASE APPROXIMATION

Thesis by

Patrick H. S. Martin

In Partial Fulfillment of the
Requirements for the Degree of
Master of Science

California Institute of Technology
Pasadena, California

(Submitted January 30, 1975)

I dedicate this work to my parents, Jorge and Judith, and to my wife, Anna. The debt of gratitude I owe them is beyond words.

ABSTRACT

Part I - Dipole Properties of Atoms and Molecules in the Random Phase Approximation

A random phase approximation (RPA) calculation and a direct sum over states is used to calculate second-order optical properties and van der Waals coefficients. A basis set expansion technique is used and no continuum-like functions are included in the basis. However, unlike other methods we do not force the basis functions to satisfy any sum-rule constraints but rather the formalism (RPA) is such that the Thomas Reiche-Kuhn sum rule is satisfied exactly. Central attention is paid to the dynamic polarizability from which most of the other properties are derived. Application is made to helium and molecular hydrogen. In addition to the polarizability and van der Waals coefficients, results are given for the molecular anisotropy of H_2, Rayleigh scattering cross sections and Verdet constants as a function of frequency. Agreement with experiment and other theories is good. Other energy weighted sum-rules are calculated and compare very well with previous estimates. The practicality of our method suggests its applications to larger molecular systems and other properties.

Part II - Photoionization Cross Sections for H_2 in the Random Phase Approximation with a Square-Integrable Basis

Total photoionization cross sections for H_2 are calculated in the Random Phase Approximation (RPA) through a numerical analytic continuation procedure applied to the polarizability for complex values

of the frequency. The representation of the polarizability that is required is obtained from a discrete set of excitation energies and oscillator strengths that satisfies the Thomas-Reich-Kuhn sum rule exactly and other energy-weighted sum rules approximately. The fact that the excitation spectrum is obtained through a solution of the RPA equations with no continuum functions added to the basis makes the method well suited for general molecular photoionization calculations. The results are compared with experiment and good agreement is found.

Part III - Oscillator Strengths for the $X^1\Sigma^+ - A^1\Pi$ System in CH^+ from the Equations of Motion Method

The equations of motion method is used to study the $X^1\Sigma^+ - A^1\Pi$ system in CH^+. In a computationally simple scheme, these calculations, which were done in modest sized basis sets, provide transition moments and oscillator strengths that agree well with the best CI calculations to date.

TABLE OF CONTENTS

Part I - Dipole Properties of Atoms and Molecules in the Random Phase Approximation

I. INTRODUCTION

Atomic and molecular polarizabilities (along with the anisotropy in the case of molecules) play a central role in the investigation of such important properties as the optical refractivity, [1] Faraday rotation, [2] Rayleigh scattering cross sections [3] and van der Waals coefficients. [4]

Experimental data on these atomic and molecular properties are far from satisfactory over a wide range of frequency values (e.g., in the vacuum uv). Experimental data are especially scarce in the case of Rayleigh scattering cross sections and depolarization ratios as well as in the rotational and vibrational Raman scattering cross section where the polarizability tensor and its variation with internuclear distance is required. [5] Although Raman scattering experiments could in principle provide a direct measurement of the polarizability anisotropy, very few values have actually been obtained.

Theoretical predictions of atomic and molecular polarizabilities are therefore useful in the analysis of available experimental data and are frequently the only available estimates of many second-order optical properties. For this reason considerable effort has been put on the theoretical and semi-empirical computation of the dynamic polarizability of atomic and molecular systems. These methods involve procedures which circumvent the infinite sum over intermediate

states in the Kramers-Heisenberg dispersion formula. One such class of methods consists of employing oscillator strength distributions and excitation energies from theoretical calculations or experiment to construct bounds for the polarizability using the theory of moments,[6] Padé approximants,[7] gaussian quadratures[8] and similar bounding techniques.[9]

An alternative approach is the semi-empirical one[10] in which oscillator strength distributions from experiment are used in the Kramers-Heisenberg dispersion formula. In cases where sufficient spectral data are available, accurate results can be obtained.

Another alternative, and this one more closely related to ours, is the variational one.[11-16] In this method the oscillator strength distributions are determined from a variational procedure subject to certain sum-rule constraints. The resulting finite spectrum does not necessarily represent an actual one (i.e., not all the poles correspond to actual states of the system) but can provide accurate values of the polarizability.

The method used in the present work is a direct sum over states procedure in which the spectrum is obtained from the random phase approximation. Next we describe our approach and apply it to several second-order optical properties of helium and molecular hydrogen. In general, agreement with previous computations and with

the available experimental data is seen to be good. The basis sets and excitation spectra used are given in Appendices II and III, respectively.

II. THEORY

Application of the semi-classical theory of the interaction of radiation with matter is known to lead to the correct results for a wide variety of phenomena of interest. Such is the case, for example, of the dynamic dipole polarizability of atomic and molecular systems, for which the formal Kramers-Heisenberg dispersion formula applies:[17]

$$\alpha(\omega) = \sum_{n\neq 0} \frac{f_{no}}{\omega_{no}^2 - \omega^2} \quad , \tag{1}$$

where the $\sum_{n\neq 0}$ is a summation over the discrete part and an integration over the continuous part of the spectrum. Atomic units are used throughout unless otherwise stated. The f_{no} and ω_{no} are the oscillator strength and the excitation energy, respectively, for the transition between state $|n\rangle$ and the ground state $|0\rangle$ of the system.

Similarly, the long range van der Waals force coefficients for the interaction between two species A and B is given by[18, 19]

$$C_{ab} = \mathcal{C}(a, b) \sum_{n\neq 0} \sum_{m\neq 0} \frac{f_{no}^{\,a} f_{mo}^{\,b}}{\omega_{no}^{\,a} \omega_{mo}^{\,b} (\omega_{no}^{\,a} + \omega_{mo}^{\,b})} \quad , \tag{2}$$

where $\mathcal{C}(a, b)$ is a constant which depends on the nature (whether atom or molecule) of the species and symmetry of the component of the polarizability to which the C_{ab} in question is related. Table AI of Appendix I gives the values of $\mathcal{C}(a, b)$ for various atom-molecule and molecule-molecule interactions. These may be easily derived from the definitions of the van der Waals coefficients in terms of

the polarizability for imaginary frequencies as given elsewhere.[10]

We assume the following definitions for the oscillator strengths and polarizability components:

$$f_{no}^{||} = \frac{2}{3}\omega_{no}\left|\langle 0|\sum_{i=1}^{N} z_i|n\rangle\right|^2 \tag{3}$$

$$f_{no}^{\perp} = \frac{4}{3}\omega_{no}\left|\langle 0|\sum_{i=1}^{N} x_i|n\rangle\right|^2 \tag{4}$$

$$\alpha_{zz}(\omega) = \alpha_{||}(\omega) = 3\sum_{n\neq 0}\frac{f_{no}^{||}}{\omega_{no}^2 - \omega^2} \tag{5}$$

$$\alpha_{xx}(\omega) = \alpha_{\perp}(\omega) = \frac{3}{2}\sum_{m\neq 0}\frac{f_{no}^{\perp}}{\omega_{mo}^2 - \omega^2} \quad . \tag{6}$$

In the above equations z points along the internuclear axis. The trace of the polarizability is given by:

$$\alpha(\omega) = \frac{1}{3}\left[2\alpha_{\perp}(\omega) + \alpha_{||}(\omega)\right] \tag{7}$$

and the anisotropy by

$$\gamma(\omega) = \alpha_{||}(\omega) - \alpha_{\perp}(\omega). \tag{8}$$

Several macroscopic properties are directly related to and determined by the microscopic atomic and molecular polarizability and anisotropy. The optical refractivity is connected to $\alpha(\omega)$ by the Lorenz-Lorentz formula:

$$\eta(\omega) - 1 = 2\pi N_0 \alpha(\omega) , \tag{9}$$

where N_0 is the number density of a dilute gas. The Verdet constant is related to the frequency derivative of the polarizability through the Becquerel formula

$$V(\omega) = \frac{1}{2c^2} \omega \frac{dn(\omega)}{d\omega} , \tag{10}$$

where c is the velocity of light. The Rayleigh scattering cross section involves both the trace of the polarizability $\alpha(\omega)$ and the anisotropy $\gamma(\omega)$:

$$\sigma(\omega) = \frac{8\pi}{9c^4} \omega^4 [3\alpha(\omega)^2 + \frac{2}{3}\gamma(\omega)^2] ; \tag{11}$$

$\alpha(\omega)$ and $\gamma(\omega)$ also completely determine the Rayleigh depolarization ratios and Raman scattering cross sections. Vibrational Raman scattering is analogously determined by the variation of the polarizability components with internuclear distance. Thus a detailed knowledge of the dipole polarizability of system conveys a wealth of information on its optical properties.

The difficulty with Eqs.(1) and (2) is that they assume a complete knowledge of the excitation spectrum of the system involved, and the determination of all the excitation energies and oscillator strengths is intractable. The cumbersome infinite summations

over the whole spectrum in Eqs. (1) and (2) are typical of the results of second-order perturbation theory. The method we employ to circumvent these summations is to replace the true spectrum by a finite number of excitation frequencies and oscillator strengths as obtained from the equations of motion (EOM) [20-22] method. The overall procedure is a direct sum over states method analogous to that of Refs. 11 and 12 (and references therein). The major difference however is the procedure for obtaining the oscillator strength distribution. A characteristic feature of our approach is that no constraints are put on the basis functions used in our calculations. Instead, ordinary Gaussian basis sets are used in the Hartree-Fock (HF) ground state calculation, and the HF orbitals provide the particle-hole basis needed for our calculation. Next we outline the EOM theory which has been fully discussed elsewhere.[20, 21]

The EOM method is a many-body approach to the calculation of excitation energies and oscillator strengths in which these quantities are calculated directly without requiring elaborate wavefunctions for the states involved. It is specifically designed for calculation of relative quantities rather than absolute energies and total wavefunctions. In the EOM method an operator O_λ^+ is defined such that

$$O_\lambda^+ |0\rangle = |\lambda\rangle, \tag{12}$$

where $|0\rangle$ is the ground state and $|\lambda\rangle$ is some excited state. O_λ^+ is then shown to satisfy the following equation of motion

$$\langle 0|[\delta O_\lambda,\ H, O_\lambda^+]|0\rangle = \omega_\lambda \langle 0|[\delta O_\lambda, O_\lambda^+]0\rangle \ , \tag{13}$$

where ω_λ is the transition frequency and δO_λ^+ is a variation in the amplitudes specifying O_λ^+. The double commutator is defined as

$$2[A, B, C] = [[A, B_-, C] + [A, [B, C]] \tag{14}$$

for any three operators A, B, and C.

If O_λ^+ is limited to single particle-hole components (1p - 1h), i.e.,

$$O_\lambda^+(SM) = \sum_{m\gamma} [Y_{m\gamma}(\lambda)\, C^+_{m\gamma}(SM) - Z_{m\gamma}(\lambda)\, C_{m\gamma}(\overline{SM})] \ , \tag{15}$$

where $C^+_{m\gamma}(SM)$ and $C_{m\gamma}(\overline{SM})$ are spin adapted particle-hole creation and annihilation operators. The amplitudes $\underset{\sim}{Y}(\lambda)$ and $Z(\lambda)$ satisfy the equation

$$\begin{pmatrix} \underset{\sim}{A} & \underset{\sim}{B} \\ -\underset{\sim}{B}^* & -\underset{\sim}{A}^* \end{pmatrix} \begin{pmatrix} \underset{\sim}{Y}(\lambda) \\ \underset{\sim}{Z}(\lambda) \end{pmatrix} = \omega_\lambda \begin{pmatrix} \underset{\sim}{D} & 0 \\ 0 & \underset{\sim}{D} \end{pmatrix} \begin{pmatrix} \underset{\sim}{Y}(\lambda) \\ \underset{\sim}{Z}(\lambda) \end{pmatrix} . \tag{16}$$

The form of the matrices $\underset{\sim}{A}$, $\underset{\sim}{B}$, and $\underset{\sim}{D}$ can be found in Refs. 20 and 21. If the Hartree-Fock approximation is used for the ground state, $\underset{\sim}{D}$ becomes the unit matrix and the RPA equations follow

$$\begin{pmatrix} \underset{\sim}{A} & \underset{\sim}{B} \\ -\underset{\sim}{B}^* & -\underset{\sim}{A}^* \end{pmatrix} \begin{pmatrix} \underset{\sim}{Y}(\lambda) \\ \underset{\sim}{Z}(\lambda) \end{pmatrix} = \omega_\lambda \begin{pmatrix} \underset{\sim}{Y}(\lambda) \\ \underset{\sim}{Z}(\lambda) \end{pmatrix} . \tag{17}$$

Higher order solutions of the EOM equations can be derived and have been used to calculate the spectra of several molecular systems with excellent agreement with experiment as well as with other theoretical results.[22] In this work however all the results are computed to the RPA level only.

In the context of the present work, the RPA has the important property of satisfying the Thomas-Reiche-Kuhn sum rule. This has been formally shown to be the case to the extent of completeness of the basis used in the calculation.[23] Actual computations have shown that reasonably sized bases provide accurate values of the S(0) sum rule (see below). As a consequence of this fact, no special sum rule constraints have to be put on the basis functions. We have also found that the other sum rules are approximately satisfied. The solution of the RPA equations in a discrete basis leads to a discrete set of oscillator strengths which are used directly to estimate $\alpha(\omega)$, Eq. (1). Some of these f_{no}'s and ω_{no}'s represent approximations to actual excited states of the system but the discrete virtual states do not correspond to actual transitions. Our expression for the polarizability is thus

$$\alpha(\omega) = \sum_{n=1}^{M} \frac{f_{no}}{\omega_{no}^2 - \omega^2} \quad , \tag{18}$$

where M is the number of states considered (the number of excitations).

The fact that there is no need to go to higher-order approximation beyond the RPA to obtain good results for $\alpha(\omega)$ and related properties, and that the equations can be solved without using any continuum-like functions, makes the present approach extremely applicable to larger molecular systems and other properties.

III. RESULTS AND DISCUSSION

Helium was calculated in three different contracted Gaussian basis sets: (11S/5p), (12S/8P) and (10S/13P) with exponents suggested by Huzinaga[24] and additional diffuse S functions and valence-like P functions.[25] Additional details of the basis sets used will be found in Appendix II. We compare the results in the three bases and show that while there is a considerable change going from (11S/5P) to (12S/8P) little is gained in going to the larger basis. In these calculations five, eight, and twelve poles of p-symmetry are obtained. The corresponding oscillator strengths and transition energies are found in Appendix III.

For molecular hydrogen we used an uncontracted (8S/5P) Gaussian basis set with exponents suggested by Huzinaga.[24] See Appendix II for further basis set information. From this calculation we have obtained 7 poles of $^1\Pi_u$ symmetry and 14 poles of $^1\Sigma_u^+$ symmetry. The resulting excitation spectrum is listed in Appendix III. The calculation was done at a fixed internuclear distance of R = 1.4 a.u. No vibrational averaging is done. Further comments on the effect of this averaging on the calculated properties will be given below.

III.1. Dynamic dipole properties

A. Helium

In Table I we compare our results for the frequency-dependent polarizability with the exact numerical solution of the time-dependent Hartree-Fock equations (to which the RPA is equivalent) given by Alexander and Gordon.[26] Agreement is excellent. The importance of this comparison is that we are able to obtain essentially exact solutions of the RPA equations using only ordinary Gaussian basis sets. This is particularly important in the present case since we are computing a quantity such as the dipole polarizability which formally involves the continuum (through the Kramers-Heisenberg formula) but using only square-integrable functions. This is a highly desirable feature of a method that is to be extended to molecular calculations.

In Table II we show the results we obtained in the three different basis sets used. $\alpha(\omega)$ was calculated at frequencies for which the exact numerical results cited above are available. The P-basis used in the (12S/8P) calculation is fairly "complete" in the sense that it provides values of $\alpha(\omega)$ which do not change appreciably in going to the larger 13P basis. For this reason the results of the larger basis are not shown in the table. Table III shows the (12S/8P) results together with the experimental values (calculated from refractivity measurements through the Lorenz-Lorentz

formula), and the moment theory bounds results of Ref. 6. Agreement of our values with experiment is good, the difference being less than 5% in all cases. Moreover this difference is reasonably constant over the range of frequencies for which experimental data are available. This suggests that if our results are scaled so that our static value agrees with the static polarizability extrapolated from the experiments, close agreement can be obtained for all other frequencies. This situation is exactly analogous to what was found by Hurst et al.[27]

Figure 1 shows the dispersion curve of $\alpha(\omega)$ of helium from zero frequency out to the second pole. The poles are marked on the axis by small triangles. The values given by this curve agree with those of Alexander and Gordon[26] even for frequencies above the first pole. Figure 2 shows a smaller section (in an expanded scale) of the dispersion curve in the region for which experiments and other calculated results are available. Our curve parallels closely the experimental points. From this it is reasonable to expect accurate values for the frequency derivative, $d\alpha(\omega)/d\omega$, required to predict Verdet constants. Here we use the Becquerel formula [Eq. (10)] which is believed to hold for atoms with reasonable accuracy. The modified Becquerel formula which is more widely used contains a empirical (frequency-independent) factor.

Table IV shows the values we obtain for the Verdet constant in the different basis sets. Again it is clear that the intermediate

size basis was enough to describe properly the property at hand. Table V shows a comparison of our (12S/8P) results with experimental and semi-empirical data as well as with other theoretical calculations. Agreement of our values with both experimental and semi-empirical data is very good, especially since Ingersol and Liebenberg[28] found that helium conforms to the Becquerel formula to within 4% only (i.e., they find 0.96 for the average value of the constant involved in the modified Becquerel formula). Our values are also in excellent agreement with a previous time-dependent coupled Hartree-Fock calculation (KCH in Table V). Even at the Lyman alpha line (1215.7 Å) our results are still in reasonably good agreement with the semi-empirical estimates. Figure 3 shows a plot of our results (solid curve), the measured Verdet coefficients and the moment theory bound results of Ref. 6.

We also compute the Rayleigh scattering cross sections for helium using Eq. (11). These are listed in Table VI for the different basis sets used. It is clear that the (12S/8P) was complete enough to describe the property. In the case of the Rayleigh scattering cross section there are no direct experimental measurements. For this reason we compute the cross sections from the experimental refractivity data and compare them with our values in Table VII. Agreement is good over a wide range of frequencies, being better at lower values. We also compare with other theoretical estimates

available. Agreement is also good. For $\lambda \leq 2500$ Å, the values listed in the last column of the table come from a time-dependent Hartree-Fock calculation. Our results agree very closely with these as they should. Figure 4 shows a plot of our results and "experimental" (in the sense explained above) data.

B. Molecular hydrogen

In Table VIII we list the results for the frequency-dependent polarizability of H_2 and compare them/ with the experimental values and/ with the values derived from a semi-empirical spectrum by Dalgarno and Victor.[10] One must be careful in comparing these results with experimental or semi-empirical results because they pertain to a fixed internuclear distance (R = 1.4 a.u. in the present case of H_2) and it has been shown recently[11, 12] that vibrational and rotational averaging can have a significant effect on the calculated properties (in some case of the order of 42%). The anisotropy for instance is particularly sensitive to the averaging mainly at higher frequencies. Except for the results of Ford and Browne,[12] no other theoretical work has included vibrational and rotational averaging effects. The values quoted from Ford and Browne's work in the table do not include averaging. Agreement with both the experimental and semi-empirical data is in general very good even at higher ω values where the averaging effects should be greater. Our agreement with other theories is excellent (including the accurate Ford and Browne results). Figure 5 shows our dispersion curve for the total polarizability out to the second pole. Figure 6 shows a more detailed view (expanded scale) of this curve together with experimental points.

Table IX shows our computed anisotropies. In this case there are practically no measurements at all (except at 6328 Å--see table) so the semi-empirical spectrum of Dalgarno and Victor[10] is used as a reliable comparison guide. The difference between our values of the anisotropy at higher frequencies and those from the model spectrum are within the possible averaging effects found by Ford and Browne.[12] In fact our result agrees very well with their unaveraged result.

Table X compares our calculated Verdet constants with experimental and semi-empirical data as well as with other theoretical results. Here the limitation of the Becquerel formula (on which our results are based) and the lack of rotational and vibrational averaging should again be kept in mind. Our results are in good agreement with the experimental values ($\leq 5\%$ in most cases). At much higher frequencies, for which experiments are unavailable, our results compare well with the semi-empirical estimates ($\sim 10\%$). Figure 7 shows a plot of our results and the experimental Verdet data. We have also computed Rayleigh scattering cross sections using our $\alpha(\omega)$ and $\gamma(\omega)$ data in Eq. (11). The results are shown in Table XI. Since no direct measurements are available we compare with the model spectrum as before. The same remarks about the averaging made before apply here again. At lower frequencies

our results are within about 10% of the semi-empirical estimates deviating more strongly at higher frequencies. This is due mainly to the lack of averaging in our anisotropy value. A plot of our results and the semi-empirical values is given in Figure 8.

III. 2. Sum rules and van der Waals coefficients

The Thomas-Reiche-Kuhn sum-rule (which the exact RPA results satisfies identically) is just one of a set of generalized energy weighted sum-rules S(k) defined by:

$$S(k) = \sum_n f_{no} (E_n - E_o)^k = \sum_n f_{no} \omega_{no}^k \quad . \tag{19}$$

For diatomic molecules this is usually broken up into two components $S^{||}(k)$ and $S^{\perp}(k)$ involving transitions polarized either parallel or perpendicular to the molecular axis. With these definitions we have

$$S^{||}(k) = 3 \sum_n f_{no}^{||} \omega_{no}^k \quad , \tag{20}$$

$$S^{\perp}(k) = \frac{3}{2} \sum_n f_{no}^{\perp} \omega_{no}^k \quad , \tag{21}$$

and

$$S(k) = \frac{1}{3} [2 S^{\perp}(k) + S^{||}(k)] \quad . \tag{22}$$

Thus the Thomas-Reiche-Kuhn sum-rule S(0) can be written for diatomic molecules as

$$S^{||}(0) = S^{\perp}(0) = S(0) = N \quad , \tag{23}$$

N being the number of electrons in the system.

We have used our oscillator strength distributions for He and H_2 to compute several of these sums and have collected them in Table XII where they are compared with previous estimates. Good agreement is found for a large number of these sum-rules. This explains in part the success of RPA theory in predicting second-order optical properties.

We have also calculated several dipole interaction coefficients through direct use of Eq. (2) and a direct sum over our discrete spectrum. These results in Table XIII agree well with the best previous estimates from Padé approximants and Gaussian quadrature procedures.[8]

IV. CONCLUSIONS

A sum-over-states procedure using a spectrum (excitation energies and oscillator strengths) from the random phase approximation in a completely square-integrable (Gaussian) basis is shown to be accurate and practical for the calculation of dipole dynamic polarizabilities and anisotropies. Applications are made to helium and molecular hydrogen. It is shown that essentially exact solutions of the RPA equations (even beyond the first pole) can be obtained using only bound-like (gaussian) basis functions on which no special constraints are imposed (e.g., sum-rule constraints). This is important since second-order optical properties formally involve the continuum.

Our dynamic polarizability results for helium are in good agreement with the exact numerical solution provided by Alexander and Gordon.[26] The results for molecular hydrogen also agree well with the best calculations available.

The RPA satisfies the Thomas-Reiche-Kuhn sum-rule exactly and we have found that it also satisfies approximately a large number of other related energy weighted sum-rules.

The accuracy of the results and the practicality and applicability of the procedure to larger molecular systems (CO, N_2, CO_2, H_2O, C_6H_6 etc.)[22] shows that the proposed method can be of wide use in the study of second-order properties and dispersion force coefficients.

Acknowledgement

One of us (P. H. S. M) thanks Marco A. C. Nascimento for his interest and helpful discussions. He thanks Anna Martin for invaluable help in the preparation of the manuscript. He also acknowledges the CNPq (Brasil) for financial support and the Physical Chemistry Department of the Universidade Federal de Rio de Janeiro for granting him a leave of absence to carry out his graduate work at Caltech.

Appendix I

Table AI - Long Range Dispersion Force Coefficients[a] Used in Eq. (2).

Interaction	$\mathcal{C}$ (a, b)
A - A	3/2
A - M ($\perp$ + $\parallel$)	3/2
A - M ($\parallel$)	3/4
A - M ($\perp$)	3/8
M ($\parallel$) - M ($\parallel$)	9/4
M ($\parallel$) - M ($\perp$)	9/8
M ($\perp$) - M ($\perp$)	9/16

---

[a] A stands for atom and M for molecule, $\perp$ for the perpendicular component and $\parallel$ for the parallel component of the molecular polarizability.

Appendix II

Basis Sets used in Calculations

Helium was calculated in three Gaussian bases: (11S/5P), (12S/8P) and (10S/13P). The (11S/5P) basis is as follows:

S Functions

Exponent	Coefficient
3293.694000	0.0046146
488.894100	0.0365754
108.772300	0.1978343
30.179900	0.8270723
9.789053	1.
3.522261	1.
1.352436	1.
0.552610	1.
0.240920	1.
0.107951	1.
0.048370	1.
0.021674	1.
0.009712	1.
0.003000	1.

P Functions

Exponent	Coefficient
1.553506	0.0710316
0.368859	-1.037338
0.119213	1.0
0.044914	1.0
0.018133	1.0
0.0073207	1.0

The (12S/8P) basis has the same S functions as the (11S/5P) above except for an additional diffuse one with exponent 0.001. The P part of the basis consists of 8 P-functions with exponents 4.5, 1.45337, 0.34627, 0.11191, 0.04216, 0.01702, 0.01127 and 0.0051.

The (10S/13P) basis has the same S components as the (11S/5P) but with the function with exponent of 0.003 deleted. The exponents for the P functions are 121.5, 40.55, 13.5, 4.5, 1.458369, 1.00, 0.34627, 0.111912, 0.042163, 0.0170230, 0.0112650, 0.0051045 and 0.0017.

Molecular hydrogen was calculated in an uncontracted (8S/5P) basis taken mostly from Huzinaga's basis.[24] Only another diffuse S function was added to the (7S/5P) basis of Huzinaga.[24] Also a d_{zz}, d_{zx} and d_{zy} function each with exponent 0.35 was placed on each hydrogen atom. On the center of the molecule an additional S function (exponent 0.0065) and a P function (exponent 0.0065) were included. The (8S/5P) part of the basis is:

S Functions

Exponent	Coefficient
213.5134	1.0
31.93095	1.0
7.15706	1.0
1.97352	1.0
0.62879	1.0
0.22444	1.0
0.087463	1.0
0.038484	1.0

P Functions

Exponent	Coefficient
2.10005	1.0
0.498629	1.0
0.161153	1.0
0.060715	1.0
0.024513	1.0

Appendix III

RPA Excitation Spectra

Excitation Energies, ω_{on}, and Oscillator Strengths, f_{on}, used in the Calculations

Helium (11S/5P)

ω_{on} (eV)	f_{on}
21.69318	0.2466
23.50479	0.0711
24.71259	0.1362
29.21289	0.4380
46.7849	0.7269
	$\Sigma f_{on} = 1.6188$

Helium (12S/8P)

ω_{on} (eV)	f_{on}
21.68579	0.2520
23.49869	0.0705
24.24010	0.0528
25.49229	0.1338
29.55789	0.3938
45.19099	0.7080
114.65388	0.3696
373.37329	0.0210
	$\Sigma f_{on} = 2.0015$

Helium (10S/13P)

ω_{on} (eV)	f_{on}
21.68559	0.2520
23.49860	0.0705
24.14690	0.0288
24.51109	0.0372
25.65469	0.1290
29.63460	0.3834
44.30089	0.6525
88.73340	0.3372
188.7334	0.0873
443.1355	0.0207
1217.095	0.0018
3672.933	0.0006
	$\Sigma f_{on} = 2.001$

Molecular Hydrogen

$H_2\ ^1\Pi_u$ States

ω_{on} (eV)	f_{on} [a]
13.08204	0.329600
14.75701	0.082748
16.40558	0.259426
23.26047	0.423587
45.29939	0.089050
47.73329	0.128098
160.01324	0.021847
	$\Sigma f_{on} = 2.0017$

H_2 $^1\Sigma_u^+$ States

ω_{on} (eV)	f_{on} [b]
12.66065	0.293237
14.59307	0.062034
15.67013	0.076577
17.54407	0.042900
20.07199	0.085979
25.11337	0.066522
33.91255	0.026622
50.64389	0.002734
55.53005	0.003803
94.04312	6.33256×10^{-4}
152.07542	4.43154×10^{-5}
218.02448	3.50420×10^{-3}
482.13574	1.14551×10^{-5}
1913.02540	2.87545×10^{-6}
	$\Sigma f_{on} = 1.994$

[a] See Eq. (3)

[b] See Eq. (4)

Table I. Frequency dependent polarizability for helium.

ω (a.u.)[d]	This work[e]	A G[a]
0.000	1.322	1.32219
0.100	1.336	1.33622
0.200	1.380	1.38056
0.300	1.462	1.46291
0.400	1.600	1.60071
0.500	1.834	1.83418
0.600	2.275	2.27585
0.700	3.435	3.43453
0.750	5.487	5.48586
$0.24\,\pi$[b]	5.832	5.83165
0.790	25.23	25.238
$0.252\,\pi$[c]	32.45	32.459
0.800	-49.57	-49.532
0.805	-16.85	-16.842

[a] See Ref. 26 of text.

[b] $0.24\,\pi \sim 0.7540$.

[c] $0.252\,\pi \sim 0.7917$.

[d] To convert from a.u. to Å use $\lambda(\text{Å}) \simeq 455.6/\omega$ (a.u.).

[e] (12S/8P) basis. See text for details.

Table II. Frequency dependent polarizability for helium $\alpha(\omega)$ (a.u.) - RPA - results in different bases.[a]

ω (a.u.)[b]	(11S/5P)	(12S/8P)	A G[c]
0.000	1.274	1.322	1.32219
0.100	1.288	1.336	1.33622
0.200	1.331	1.380	1.38056
0.300	1.411	1.462	1.46291
0.400	1.546	1.600	1.60071
0.500	1.773	1.834	1.83418
0.600	2.204	2.275	2.27585
0.700	3.333	3.435	3.43453
0.750	5.323	5.487	5.48586
0.24π[d]	5.656	5.832	5.83165
0.790	23.74	25.23	25.238
0.252π[e]	30.15	32.45	32.459
0.800	-54.18	-49.57	-49.532
0.805	-17.26	-16.85	-16.842

[a] See text for description of basis set.

[b] To convert from a.u. to Å, use $\lambda(\text{Å}) \simeq 455.6/\omega(\text{a.u.})$.

[c] Reference 26.

[d] $0.24\pi \sim 0.7540$.

[e] $0.252\pi \sim 0.7917$.

Table III. Frequency dependent polarizability of helium. Comparison with other results

λ (Å)	Experimental[a]	This work[c]	PWL[b]
20587.0	1.3868	1.3225	-
15300.0	1.3873	1.3228	-
14756.0	1.3876	1.3229	-
10142.0	1.3892	1.3244	-
9227.0	1.3899	1.3249	1.388
8266.8	1.3908	1.3258	1.389
7247.2	1.3923	1.3271	1.390
5462.2	1.3971	1.3313	1.395
4801.3	1.4004	1.3342	1.398
4359.0	1.4009	1.3369	1.401
4047.0	1.4037	1.3394	1.404
3907.0	1.4052	1.3407	-
3664.0	1.4082	1.3434	1.408
3342.0	1.4133	1.3479	-
3132.0	1.4175	1.3517	1.417
3022.0	1.4200	1.3540	-
3968.0	1.4215	1.3552	-
2926.0	1.4226	1.3562	-
2894.0	1.4236	1.3570	-
2753.0	1.4279	1.3609	1.423

Table III (continued)

[a] Experimental refractivity data from: C. R. Mansfield and E. R. Peck, J. Opt. Soc. Am. 59, 199 (1969); C. Cuthbertson and M. Cuthbertson, Proc. Roy. Soc. (London) 135, 40 (1932).

[b] See Ref. 6 of text.

[c] (12S/8P) basis. See text for details.

Table IV. Verdet constant for helium - RPA.

Comparison of different bases.

λ (Å)	$V(\omega)^a$ (11S/5P)[b]	$V(\omega)^a$ (12S/8P)[b]
9875.	0.1459	0.1497
9000.	0.1759	0.1804
8500.	0.1974	0.2025
8000.	0.2230	0.2288
7500.	0.2540	0.2606
7000.	0.2920	0.2995
6500.	0.3392	0.3480
6000.	0.3990	0.4093
5780.	0.4304	0.4415
5500.	0.4761	0.4884
5460.	0.4833	0.4957
5000.	0.5782	0.5932
4500.	0.7174	0.7359
4360.	0.7655	0.7853
4000.	0.9143	0.9379
3635.	1.115	1.144
2500.	2.467	2.530
1215.7[c]	14.25	14.61
1000.	26.56	27.24

Table IV (continued)

[a] In units of microminutes. Oersted^{-1} cm^{-1} (at 0°C and 1 atm).

[b] See Text for description of basis sets. The results for the (10S/13P) basis are identical to the (12S/8P) to 4 significant figures.

[c] Lyman alpha radiation.

Table V. Verdet constants for helium - RPA.

Comparison with other work.

λ (Å)	Experimental[a]	Semi empirical[b]	KCH[c]	This work[f]	PWL[d]
9875.	-	0.161	0.1499	0.1497	-
9000.	0.205	0.194	0.1807	0.1804	-
8500.	0.221	0.218	0.2027	0.2025	0.224
8000.	0.246	0.246	0.2290	0.2288	0.253
7500.	0.283	0.281	0.2609	0.2606	0.288
7000.	0.325	0.323	0.2999	0.2995	0.332
6500.	0.376	0.375	0.3484	0.3480	0.385
6000.	0.441	0.441	0.4098	0.4093	0.453
5780.	0.474	0.476	0.4421	0.4415	-
5500.	0.523	0.526	0.4890	0.4884	0.540
5460.	0.531	0.534	0.4963	0.4957	-
5000.	0.638	0.639	0.5939	0.5931	0.657
4500.	0.800	0.793	0.7368	0.7359	0.815
4360.	0.854	0.846	0.7862	0.7853	-
4000.	1.011	1.01	0.9390	0.9379	1.039
3635.	1.249	1.23	1.145	1.144	-
2500.	-	2.73	2.533	2.530	-
1215.7[e]	-	15.5	14.28	14.61	-
1000.	-	27.5	25.28	27.24	-

Table V (continued)

[a] See Ref. 29 of text.

[b] A. Dalgarno and A. E. Kingston, Proc. Roy. Soc. (London) A259, 424 (1960).

[c] See Ref. 27 of text.

[d] See Ref. 6 of text.

[e] Lyman α radiation.

[f] Units of microminutes. $Oe^{-1} \cdot cm^{-1}$ (at 0°C and 1 atm).

Table VI. Rayleigh scattering cross sections for helium - RPA. Comparison of different bases.

λ (Å)[c]	$\sigma(\omega)$[a] (11S/5P)[b]	$\sigma(\omega)$[a] (8S/13P)[b]
∞	0.0	0.0
20586.0	0.002593	0.002789
15300.0	0.008507	0.009151
14756.0	0.009833	0.01058
10142.0	0.04416	0.04750
9227.0	0.06453	0.06941
8266.8	0.1003	0.1079
7247.2	0.1701	0.1830
5462.2	0.5305	0.5706
4801.3	0.8926	0.9600
4359.0	1.319	1.419
4047.0	1.782	1.917
3907.0	2.056	2.211
3664.0	2.669	2.870
3342.0	3.882	4.174
3132.0	5.061	5.442
3022.0	5.859	6.300
2968.0	6.309	6.783
2926.0	6.689	7.192
2894.0	6.998	7.524
2753.0	8.595	9.240

Table VI (continued)

[a] In units of 10^{-28} cm^2.

[b] See text for description of basis sets. The (10S/13P) results are identical to the (12S/8P) values to 4 significant digits.

[c] Wavelengths at which experimental refractivity data are available.

Table VII. Rayleigh scattering cross sections for helium - RPA. Comparison with other work.

λ (Å)	$\sigma(\omega)$[a] Experimental[c]	$\sigma(\omega)$[a] This work[d]	$\sigma(\omega)$[a] Other theories
20587.0	0.003069	0.002789	-
15300.0	0.01006	0.009151	-
14756.0	0.01164	0.01058	-
10142.0	0.05226	0.04750	-
9227.0	0.07638	0.06941	0.0761[b]
8266.8	0.1187	0.1079	0.118[b]
7247.2	0.2014	0.1830	0.201[b]
5462.2	0.6284	0.5706	0.626[b]
4801.3	1.058	0.9600	1.054[b]
4359.0	1.558	1.419	1.558[b]
4047.0	2.105	1.917	2.104[b]
3907.0	2.429	2.211	-
3664.0	3.153	2.870	3.153[b]
3342.0	4.589	4.174	-
3132.0	5.985	5.442	5.980[b]
3022.0	6.929	6.300	-
2968.0	7.462	6.783	-
2926.0	7.913	7.192	-
2894.0	8.280	7.524	-
2753.0	10.17	9.240	10.17[b]
2500.0	-	13.76	13.74[e] (15.)[f]
2000.0	-	35.03	34.98[e] (138.)[f]

Table VII (continued)

λ (Å)	$\sigma(\omega)$[a] Experimental[c]	$\sigma(\omega)$[a] This work[d]	$\sigma(\omega)$[a] Other Theories
1500.	-	121.7	121.5[e] (133.)[f]
1216.	-	318.3	317.9[e] (353.)[f]
1000.	-	841.7	840.7[e] (951.)[f]
800.	-	3099.	3096.[e] (3590.)[f]
700.	-	8654.	8650.[e] (10700.)[f]

---

[a] In units of 10^{-28} cm^2.

[b] See Ref. 6 of text.

[c] Calculated from experimental refractivity data (which provides the necessary polarizability values).

[d] (12S/8P) basis see text for details.

[e] M. J. Jamieson, in Quantum Mechanics, the First Fifty Years, W. C. Price, S. S. Chissick and T. Ravensdale, editors (John Wiley, 1973).

[f] Y. M. Chan and A. Dalgarno, Proc. Roy. Soc. (London) 85, 227 (1965).

Table VIII. Frequency dependent polarizability for H_2 (R = 1.4 a.u.). Comparison with experimental and other theories. Full polarizability $\alpha(\omega)$ in a.u.

λ (Å)	Experimental [a]	Model spectrum [b]	This work	FB [c]	PWL [d]
∞	5.437	5.450	5.235	5.18	5.437
6328.0	5.554	5.554	5.331	5.28	-
5462.3	5.582	5.591	5.365	5.31	5.588
4556.0	-	5.655[e]	5.424	-	-
4359.6	5.667	5.675	5.443	5.39	5.668
4079.0	5.701	5.708	5.474	-	5.704
3342.4	5.840	5.845	5.600	-	5.832
3037.3	-	5.937[e]	5.685	-	-
2968.1	5.960	5.963	5.708	5.65	5.948
2753.6	6.055	6.056	5.794	-	6.036
2379.1	6.303	6.299	6.017	-	-
2302.9	6.384	6.368	6.079	6.01	6.332
2278.0	-	6.392[e]	6.101	-	-
1935.8	6.868	6.865	6.530	-	6.799
1854.6	7.035	7.035	6.683	6.59	6.959
1822.4	-	7.112[e]	6.752	-	-
1700.0	-	7.471	7.071	-	-
1600.0	-	7.872	7.424	7.31	-
1500.0	-	8.431	7.908	-	-
1400.0	-	9.262	8.610	8.44	-
1300.0	-	10.62	9.714	-	-
1215.7	12.8	12.76	11.29	11.02	-

Table VIII (continued)

[a] From refractivity data: (1) J. Kock, Arkiv. Math. Astron. Fysik. 8, 20 (1912) and M. Kirn, An. Physik 64, 566 (1912); (2) $\lambda = \infty$ Å, H. Schuler and K. L. Wolf, Z. Physik 34, 343 (1925); (3) λ = 6328 Å, N. J. Bridge and A. D. Buckingham, J. Chem. Phys. 40, 2733 (1964). Proc. Roy. Soc. (London) A295, 334 (1966); (4) λ = 1215.7 Å (Lyman α), P. Gill and D. W. O. Heddle, J. Opt. Soc. Am. 53, 848 (1963).

[b] Model semi-empirical spectrum of H_2 constructed by G. A. Victor and A. Dalgarno, J. Chem. Phys. 50, 2535 (1969).

[c] Direct sum-over-states calculation of Ref. 12 of text.

[d] Padé approximants calculation of P. W. Langhoff and M. Karplus, Ref. 7.

[e] Calculated from the model spectrum of G. A. Victor and A. Dalgarno, J. Chem. Phys. 50, 2535 (1969).

Table IX. Frequency dependent anisotropy for H_2 (R = 1.4 a.u.). Comparison with other theories. (γ (ω) given in a.u.)

λ (Å)	Model spectrum[a]	This work	FB[b]	PWL[c]
∞	2.029	1.865	1.84	1.826
6328.0	2.092	1.919	1.90	-
5462.3	2.115	1.938	1.92	-
4556.0	2.155	1.972	-	1.930
4359.6	2.168	1.982	1.96	-
4079.0	2.188	2.000	-	-
3342.4	2.274	2.073	-	-
3037.3	2.333	2.122	-	2.074
2968.1	2.350	2.136	2.11	-
2753.6	2.410	2.186	-	-
2379.1	2.569	2.319	-	-
2302.9	2.615	2.357	2.32	-
2278.0	2.631	2.370	-	2.311
1935.8	2.958	2.637	-	-
1854.6	3.080	2.734	2.69	-
1822.4	3.136	2.779	-	2.703
1700.0	3.401	2.988	-	-
1600.0	3.710	3.226	3.16	-
1500.0	4.159	3.564	-	-
1400.0	4.871	4.077	3.95	-
1300.0	6.158	4.939	-	-
1215.7	8.495	6.285	6.12	-

Table IX (continued)

[a] Model semi-empirical spectrum of H_2 constructed by G. A. Victor and A. Dalgarno, J. Chem. Phys. 50, 2535 (1969).

[b] Direct sum-over-states calculation of Ref. 12 of text. Unaveraged results shown for comparison. See text.

[c] Moment theory bounds results of Ref. 6 of text.

Table X. Verdet constants V (ω)[a] of H_2 (R = 1.4 a.u.)

λ (Å)	Experiment[b]	Model spectrum[c]	This work	PWL[d]
∞	-	0.	0.	-
9875.	2.11	2.15	1.99	-
9000.	2.53	2.59	2.41	-
8500.	2.83	2.91	2.71	2.81
8000.	3.18	3.30	3.07	3.18
7500.	3.59	3.77	3.50	3.64
7000.	4.14	4.35	4.04	4.19
6500.	4.88	5.07	4.71	4.89
6000.	5.81	5.99	5.56	5.78
5893.	6.03	6.22	5.77	-
5780.	6.27	6.48	6.01	-
5500.	6.94	7.20	6.68	6.93
5460.	7.06	7.31	6.78	-
5000.	8.55	8.82	8.17	8.49
4500.	10.7	11.1	10.2	10.65
4360.	11.4	11.9	11.0	-
4000.	13.8	14.3	13.3	13.78
3635.	17.2	17.8	16.4	-
3342.4	-	21.6	19.9	-
2500.	-	44.3	40.5	-
2000.	-	84.1	76.0	-

Table X (continued)

[a] In units of microminutes. Oersted^{-1} cm^{-1} (at 0°C and 1 atm).

[b] Ref. 29.

[c] Model semi-empirical spectrum of H_2 constructed by G. A. Victor and A. Dalgarno, J. Chem. Phys. 50, 2535 (1969). With the exception of the points at $\lambda = \infty$A and $\lambda = 3342.4$ Å the values were calculated from their spectrum.

[d] Moment theory bounds results of Ref. 6.

Table XI. Rayleigh scattering cross sections for H_2. (R = 1.4 a.u.)
$\sigma(\omega)$[a]

λ (Å)	Model Spectrum[b]	This work	PWL[c]
∞	0.	0.	-
6328.0	0.0569	0.0523	-
5462.3	0.104	0.0953	0.1
4359.6	0.264	0.242	0.264
4079.0	0.348	0.319	0.348
3342.4	0.811	0.742	0.809
2968.1	1.36	1.24	1.35
2753.6	1.89	1.73	1.88
2379.1	3.68	3.35	-
2302.9	4.29	3.89	4.24
1935.8	10.0	9.02	9.82
1854.6	12.5	11.2	12.2
1700.0	20.0	17.8	-
1600.0	28.4	25.1	-
1500.0	42.4	37.0	-
1400.0	68.0	58.1	-
1300.0	122.	100.	-
1215.7	235.	179.	-

[a] In units of 10^{-26} cm^2.

[b] Model semi-empirical spectrum of H_2 constructed by G. A. Victor and A. Dalgarno, J. Chem. Phys. 50, 2535 (1969).

[c] Moment theory bounds results of Ref. 6.

Table XII. Sum rules S(k) for helium and molecular hydrogen.

System	S (2)	S (1)	S (0)	S (-1)	S (-2)	S (-4)	S (-6)
He	30.37[a]	4.126[a]	2.001	1.478	1.322	1.386	1.730
	(30.3325)[b]	(4.0837)[b]	(2)[c]	(1.505)[b]	(1.3838)[d]	(1.550)[d]	(2.066)[d]
H_2	2.447	1.666	1.999	3.053	5.234	18.25	71.29
	(3.6929)[e]	(1.7035)[e]	(2)[c]	(3.1671)[f]	(5.439)[d]	(20.02)[d]	(81.61)[d]
$H_2^{\parallel}$	1.639	1.330	1.994	3.478	6.478	25.03	104.5
	(0.82)[g]	(1.214)[g]	(2)[c]	(3.4452)[h]	(6.3517)[h]	(27.55)[g]	
$H_2^{\perp}$	2.851	1.835	2.002	2.841	4.613	14.86	54.66
	(1.93)[g]	(1.674)[g]	(2)[c]	(2.8264)[e]	(4.750)[e]	(15.67)[g]	

[a] These values pertain to the (10S/13P) calculation on He (see text for details).

[b] C. L. Pekeris, Phys. Rev. 112, 1649 (1958).

[c] Exact value.

[d] P. W. Langhoff and M. Karplus, J. Opt. Soc. Am. 59, 863 (1969).

[e] W. Kolos and L. Wolnievicz, J. Chem. Phys. 41, 3663 (1964); ibid. 46, 1426 (1967).

Table XII (continued)

[f] R. Kamikawai, T. Watanabe and A. Amemiya, Phys. Rev. 184, 303 (1969).

[g] G. A. Victor and A. Dalgarno, J. Chem. Phys. 50, 2535 (1969).

[h] Ref. 12.

Table XIII. Van der Waals force coefficients for He and H_2 interactions[a]

Interaction	He - He	He - H_2[b]	He - $H_2(\parallel)$	He - $H_2(\perp)$	$H_2(\parallel)$ - $H_2(\parallel)$	$H_2(\perp)$ - $H_2(\parallel)$	$H_2(\perp)$ - $H_2(\perp)$
This work	1.374	3.796	0.748	0.575	2.749	2.069	1.563
Other work	1.375[c]	3.794[d]	0.746[c]	0.5755[c]	2.732[c]	2.063[c]	1.564[c]

[a] Entries refer to the C_{ab}'s defined in text (Eq. (2)).

[b] Full polarizability used for H_2.

[c] P. W. Langhoff, R. G. Gordon and M. Karplus, J. Chem. Phys. 55, 2126 (1971).

[d] Computed from data in Ref. c above according to Eq. (6a) of that work.

References

1. S. A. Korff and G. Breit, Rev. Mod. Phys. 4, 471 (1932).
2. R. Serber, Phys. Rev. 41, 489 (1932).
3. I. L. Fablenski, Molecular Scattering of Light, (Plenum, New York, 1968).
4. H. B. G. Casimir and D. Polder, Phys. Rev. 73, 360 (1948); A. Dalgarno, Advan. Chem. Phys. 12, 143 (1967).
5. The Raman Effect, edited by A. Anderson (Dekker, New York, 1971).
6. P. W. Langhoff, J. Chem. Phys. 57, 2604 (1972).
7. P. W. Langhoff and M. Karplus, J. Chem. Phys. 52, 1435 (1970).
8. See P. W. Langhoff, R. G. Gordon, and M. Karplus, J. Chem. Phys. 55, 2126 (1971).
9. See P. T. Gee and K. T. Tang, Phys. Rev. A. 7, 1863 (1973) and the references therein. See also Ref. 8 above, footnote 28.
10. See for instance A. E. Kingston, J. Opt. Soc. Am. 54, 1145 (1964); G. A. Victor and A. Dalgarno, J. Chem. Phys. 50, 2535 (1969).
11. A. Dalgarno, A. L. Ford, and J. C. Browne, Phys. Rev. Lett. 27, 1033 (1971).
12. A. L. Ford and J. C. Browne, Phys. Rev. A. 7, 418 (1973).
13. M. Karplus and H. J. Kolker, J. Chem. Phys. 39, 1413 (1963).
14. M. Karplus and H. J. Kolker, J. Chem. Phys. 41, 3955 (1964).
15. H. J. Kolker and H. H. Michels, J. Chem. Phys. 43, 1027 (1965).
16. A. Dalgarno and S. T. Epstein, J. Chem. Phys. 50, 2837 (1969).

17. J. C. Salter, Quantum Theory of Atomic Structure, Vol. I, page 154 (McGraw-Hill, New York, 1969).

18. See for example J. O. Hirschfelder and W. J. Meath, Adv. Chem. Phys. 12, 3 (1967).

19. A. Dalgarno and W. D. Davison, Advan. Atom. Mol. Phys. 2, 1 (1966); also A. Dalgarno, Adv. Chem. Phys. 12, 143 (1967).

20. T. Shibuya and V. McKoy, Phys. Rev. A2, 2208 (1970).

21. T. Shibuya, J. Rose and V. McKoy, J. Chem. Phys. 58, 500 (1973).

22. T. Shibuya and V. McKoy, Phys. Rev. A2, 2208 (1970); J. Rose, T. Shibuya and V. McKoy, J. Chem. Phys. 58, 74 (1973); J. Rose, T. Shibuya and V. McKoy, J. Chem. Phys. (to appear April 1974); D. L. Yeager and V. McKoy, J. Chem. Phys. (to appear April 1974).

23. R. A. Harris, J. Chem. Phys. 50, 3947 (1969); see also D. J. Thouless, Nucl. Phys. 22, 781 (1961).

24. S. Huzinaga, J. Chem. Phys. 42, 1293 (1965).

25. C. W. McCurdy, Jr. and V. McKoy, J. Chem. Phys. (to be published).

26. M. H. Alexander and R. G. Gordon, J. Chem. Phys. 56, 3823 (1972).

27. V. G. Kaveeshwar, K. T. Chung and R. P. Hurst, Phys. Rev. 172, 35 (1968).

28. L. R. Ingersoll and D. H. Liebenberg, J. Opt. Soc. Am. 44, 566 (1954); ibid. 46, 538 (1956).

FIGURE CAPTIONS

Figure 1. Dispersion of the dipole polarizability of He for frequencies up to the second pole.

Figure 2. Frequency-dependent polarizability of He. Comparison of this work with experiment (small x's) and results from Ref. 6 (small circles).

Figure 3. Verdet constants of He (in units of microminutes. Oe^{-1}. cm^{-1} at 0°C and 1 atm.). Comparison of this work with experiment (small x's) and results of Ref. 6 (small circles).

Figure 4. Rayleigh scattering cross sections of He (in units of 10^{-28} cm^2). Comparison of this work with experiment and results of Ref. 6.

Figure 5. Dispersion of $\alpha(\omega)$ for H_2 (R = 1.4 a.u.).

Figure 6. Frequency-dependent polarizability of H_2 (R = 1.4 a.u.). Comparison of this work with experiment (x in the figure) and results of Ref. 6 (marked o).

Figure 7. Verdet constants of H_2 (R = 1.4 a.u.). Comparison of this work with experiment (x in the figure) and results of Ref. 6 ('o'). (Units are microminutes. Oe^{-1}. cm^{-1} at 0°C and 1 atm.)

Figure 8. Rayleigh scattering cross sections for H_2 (R = 1.4 a.u.). Comparison of this work with semi-empirical estimates and results of Ref. 6 (x and o , respectively, in the figure). Units are 10^{-28} cm^2.

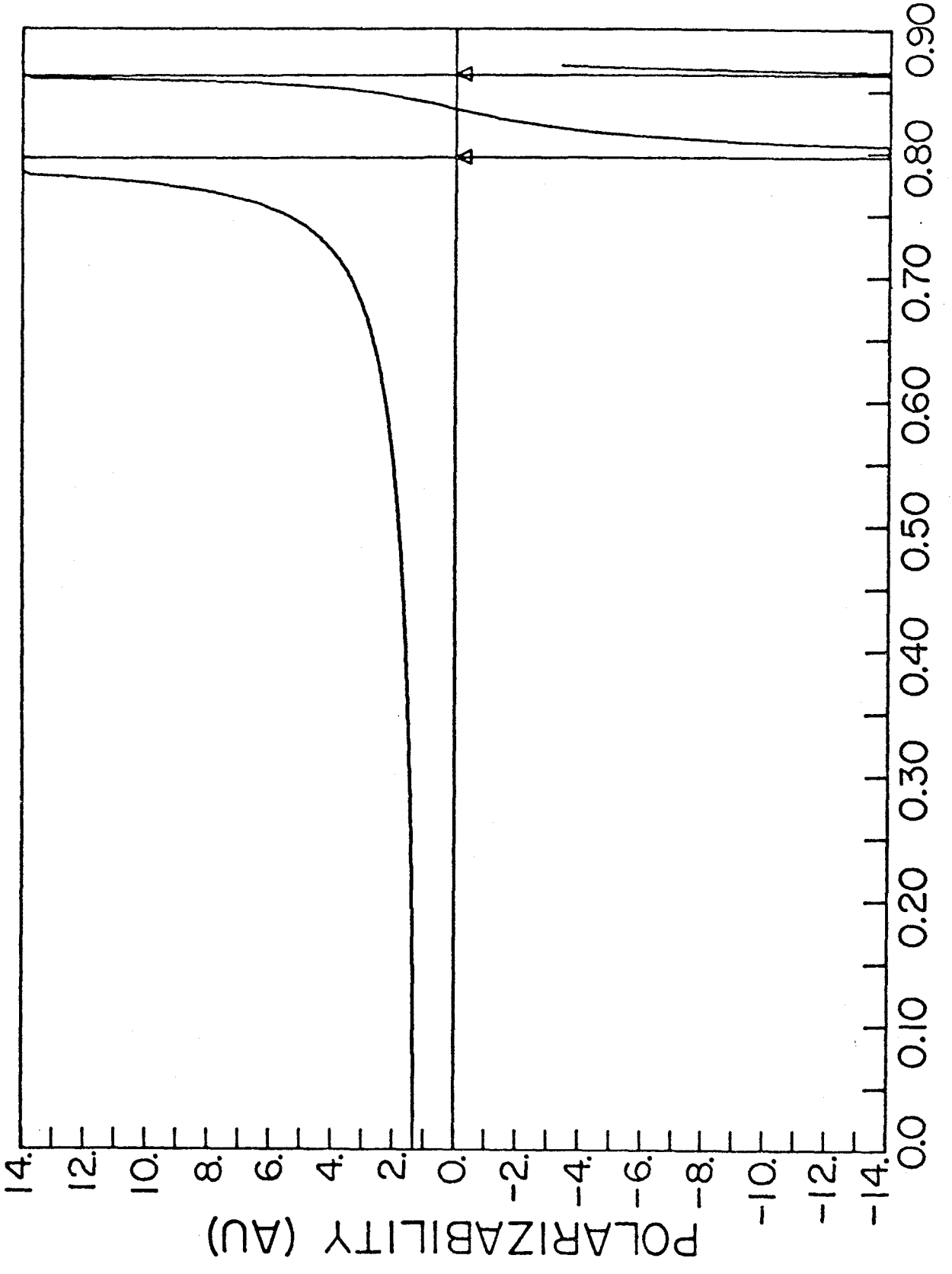
FREQUENCY (AU)
0.0
0.10
0.20
0.30
0.40
0.50
0.60
0.70
0.80
0.90
POLARIZABILITY (AU)
14.
12.
10.
8.
6.
4.
2.
0.
-2.
-4.
-6.
-8.
-10.
-12.
-14.

Figure 1.

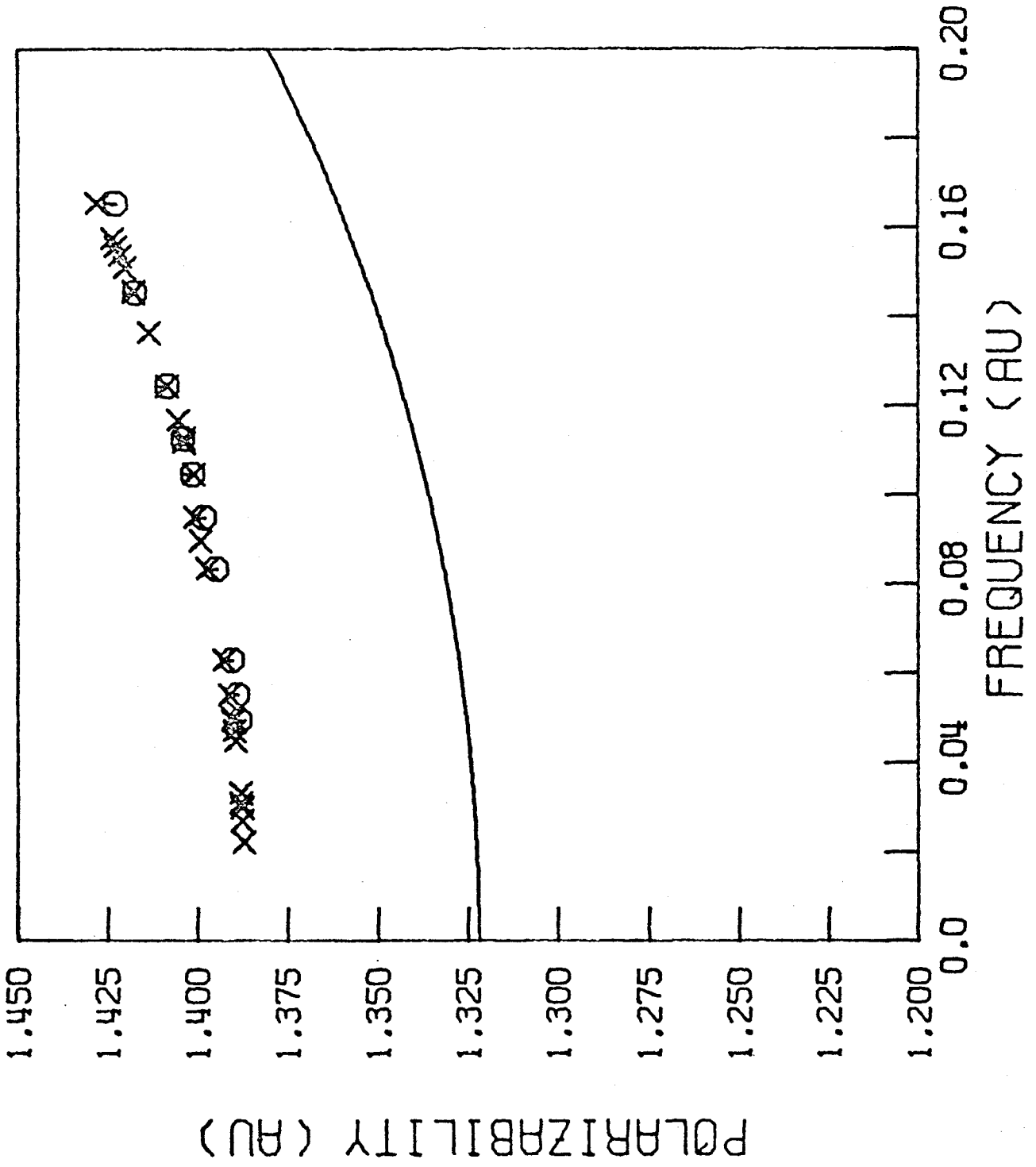
POLARIZABILITY (AU)
1.450
1.425
1.400
1.375
1.350
1.325
1.300
1.275
1.250
1.225
1.200
0.0
0.04
0.08
0.12
0.16
0.20
FREQUENCY (AU)

Figure 2.

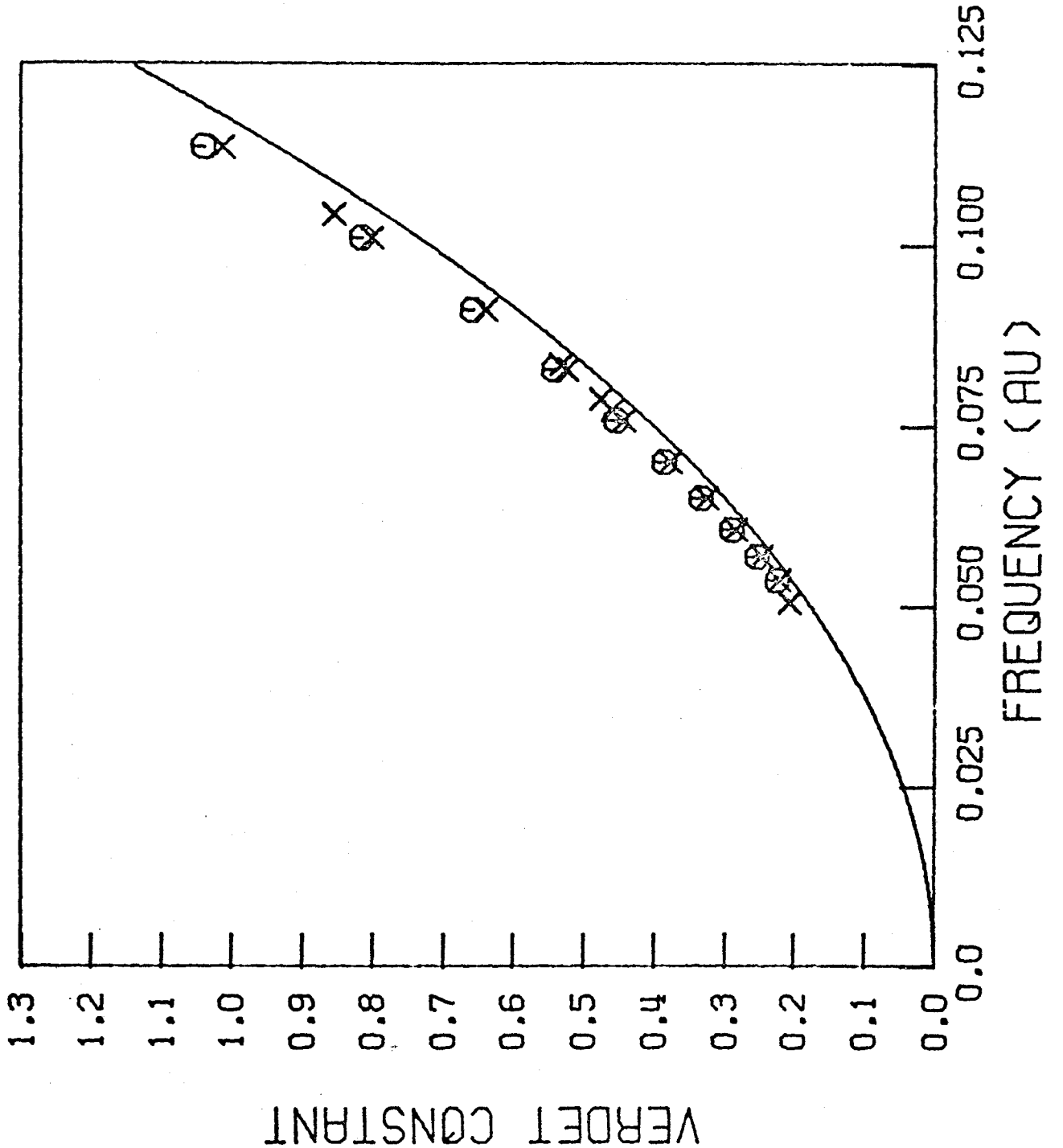
VERDET CONSTANT
1.3
1.2
1.1
1.0
0.9
0.8
0.7
0.6
0.5
0.4
0.3
0.2
0.1
0.0
0.0
0.025
0.050
0.075
0.100
0.125
FREQUENCY (AU)

Figure 3.

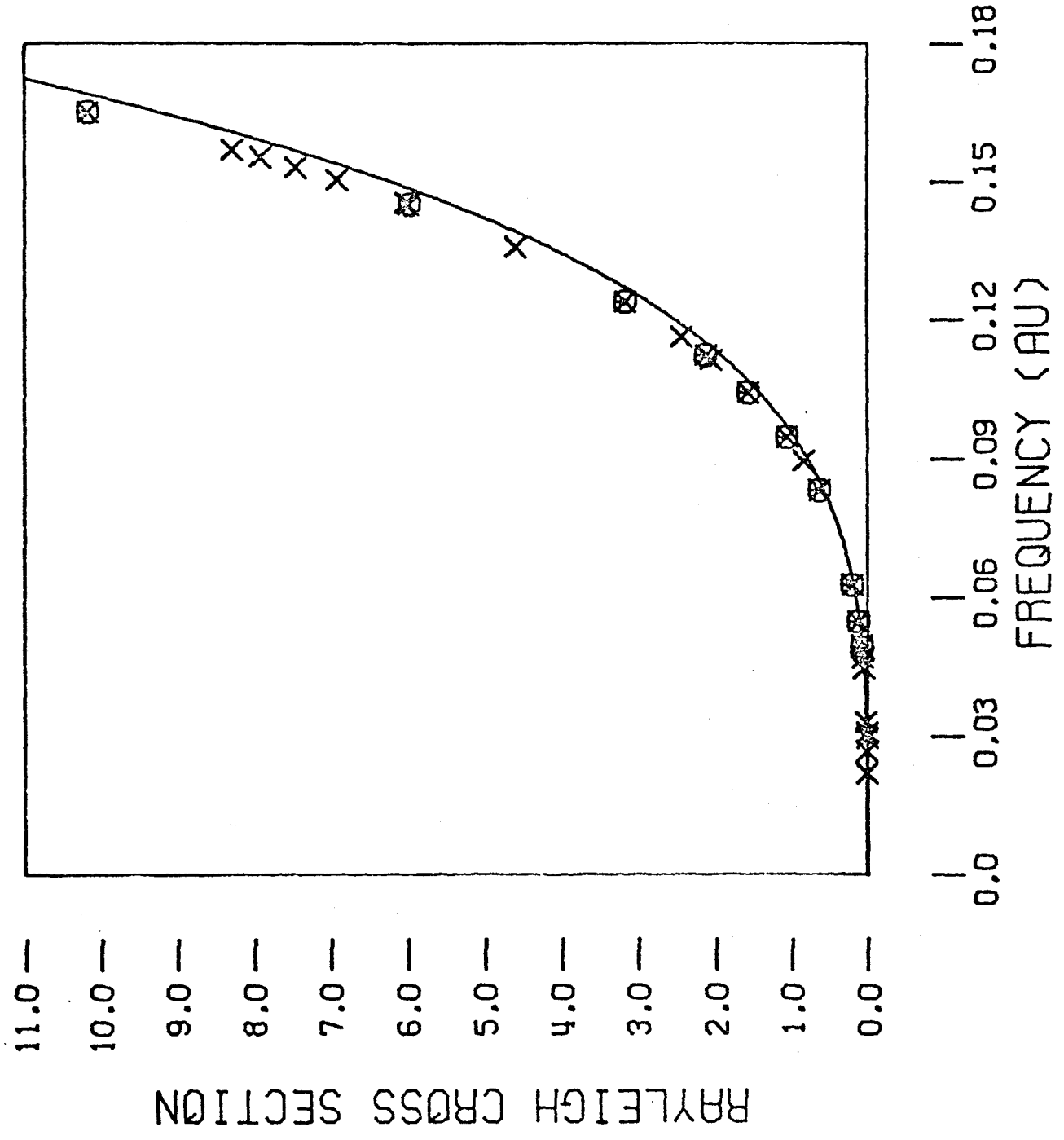
RAYLEIGH CROSS SECTION
11.0
10.0
9.0
8.0
7.0
6.0
5.0
4.0
3.0
2.0
1.0
0.0
0.0
0.03
0.06
0.09
0.12
0.15
0.18
FREQUENCY (AU)

Figure 4.

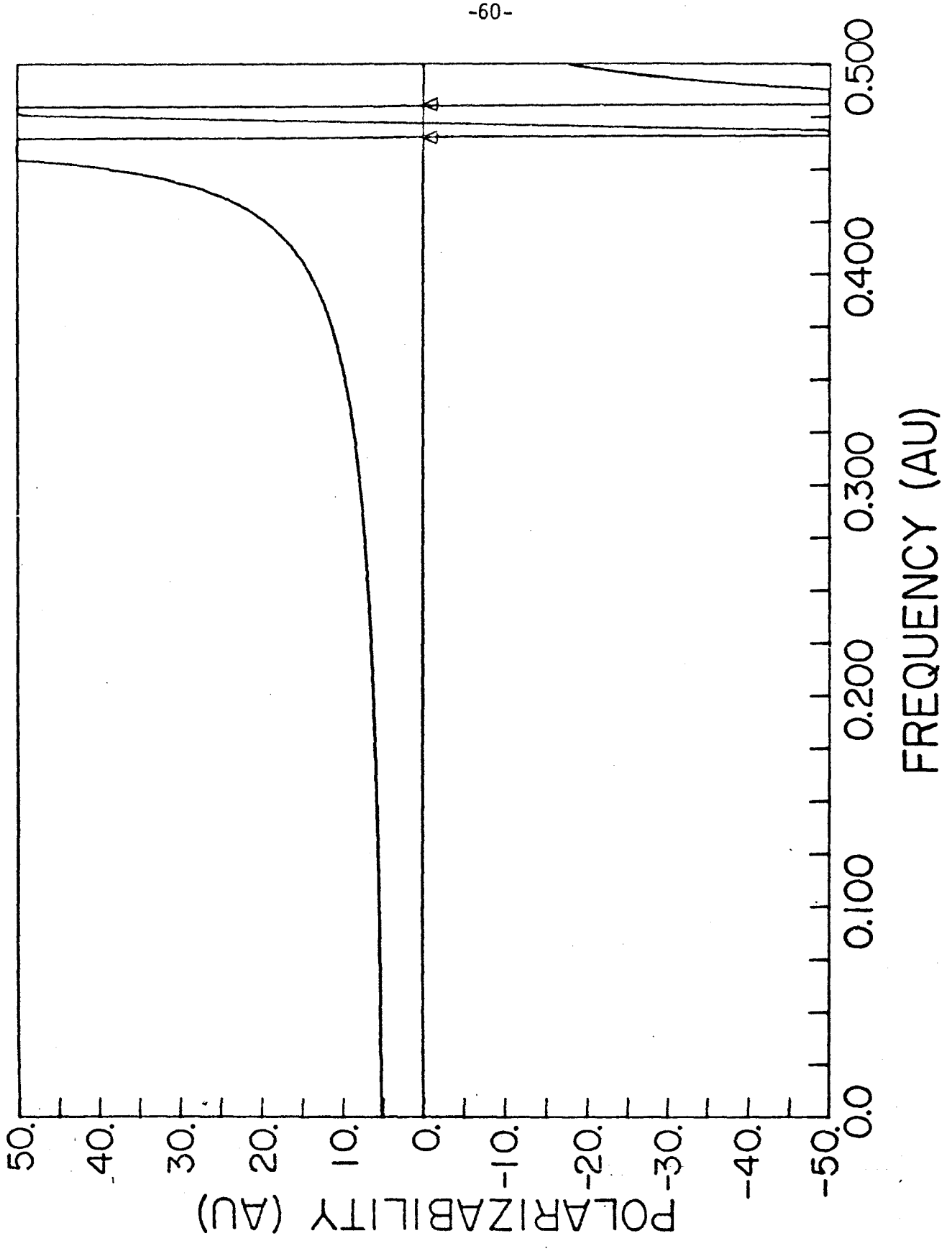
POLARIZABILITY (AU)
50.
40.
30.
20.
10.
0.
-10.
-20.
-30.
-40.
-50.
0.0
0.100
0.200
0.300
0.400
0.500
FREQUENCY (AU)

Figure 5.

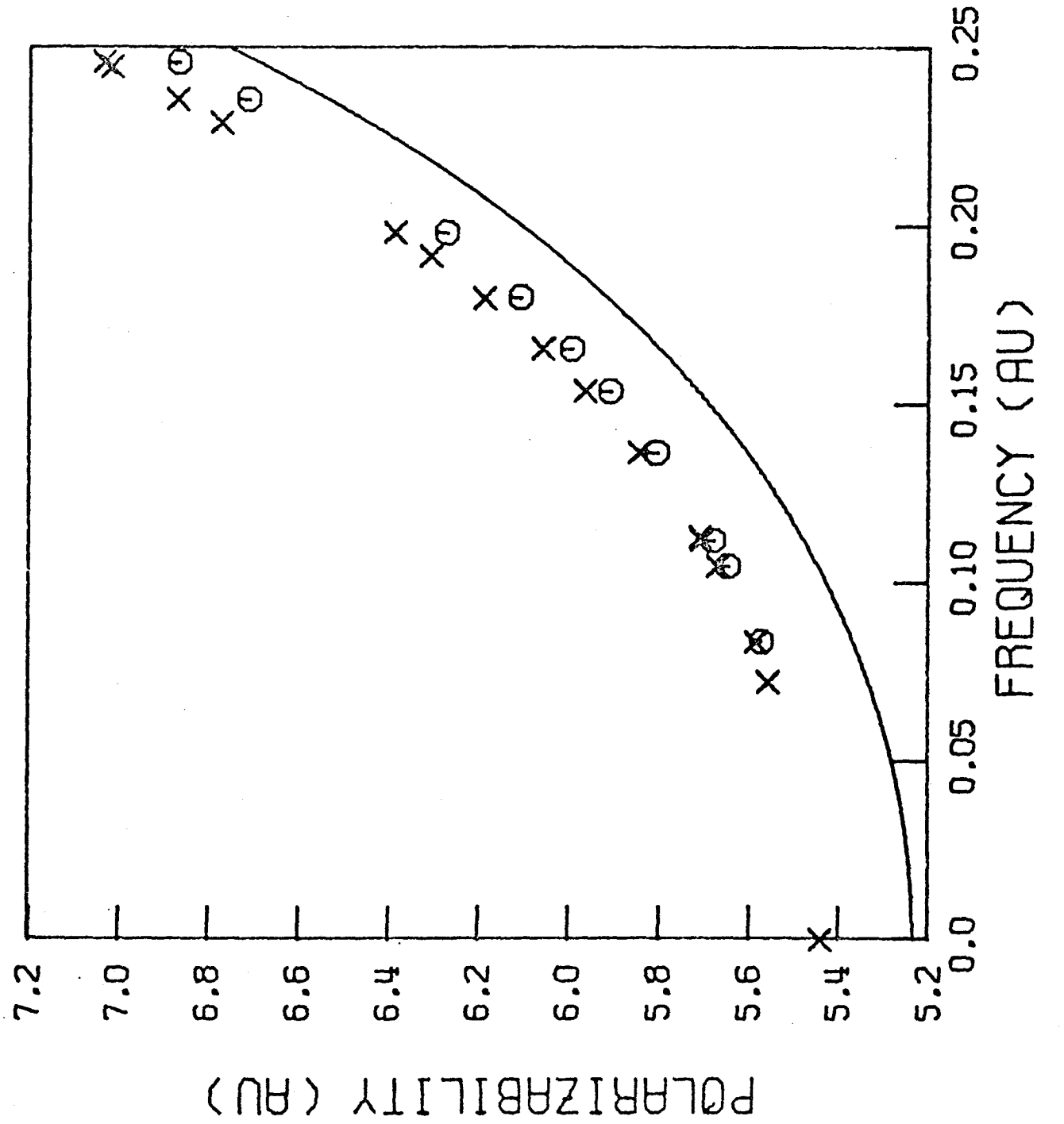
POLARIZABILITY (AU)
7.2
7.0
6.8
6.6
6.4
6.2
6.0
5.8
5.6
5.4
5.2
0.0
0.05
0.10
0.15
0.20
0.25
FREQUENCY (AU)

Figure 6.

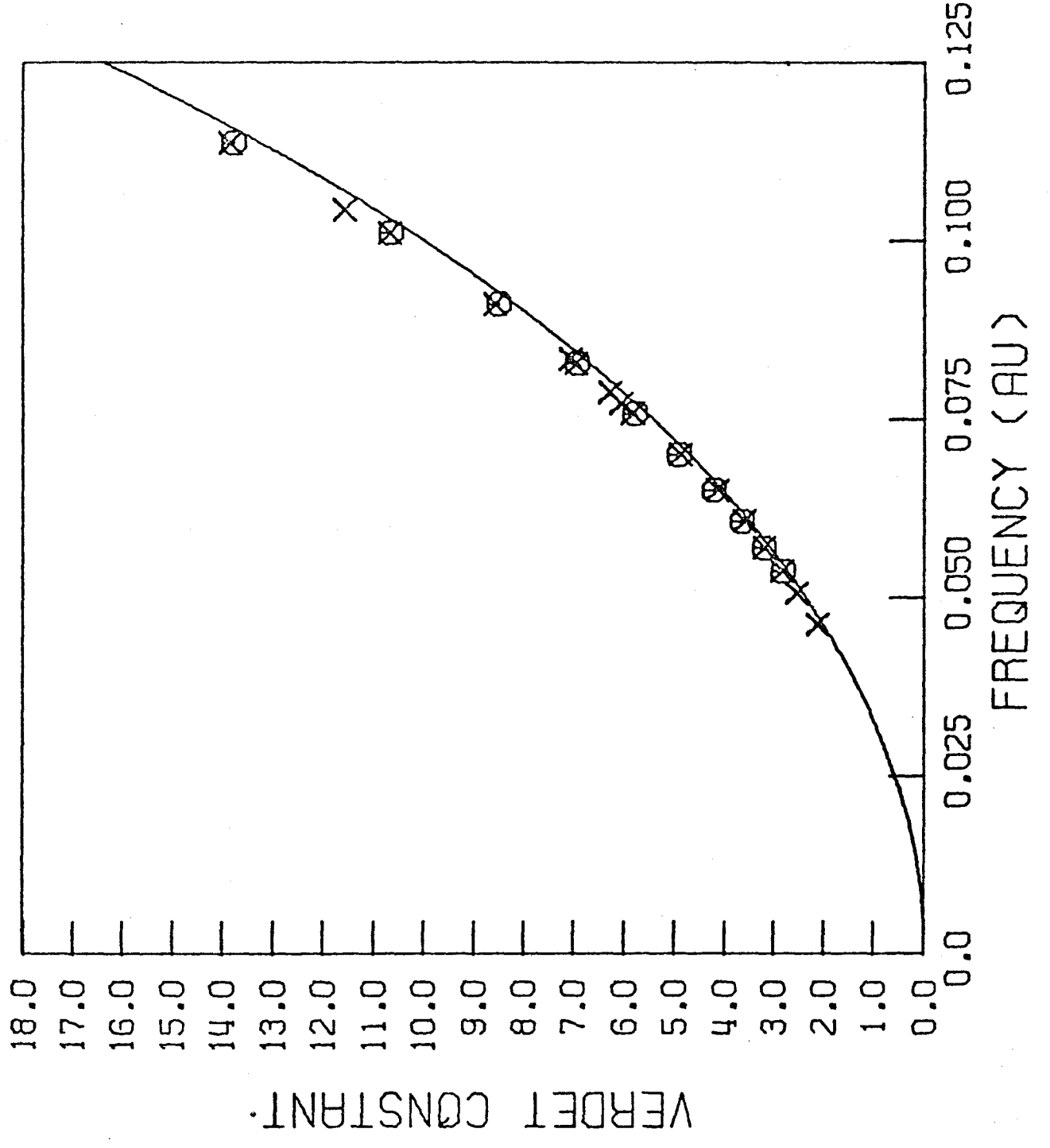
VERDET CONSTANT
18.0
17.0
16.0
15.0
14.0
13.0
12.0
11.0
10.0
9.0
8.0
7.0
6.0
5.0
4.0
3.0
2.0
1.0
0.0
0.0
0.025
0.050
0.075
0.100
0.125
FREQUENCY (AU)

Figure 7.

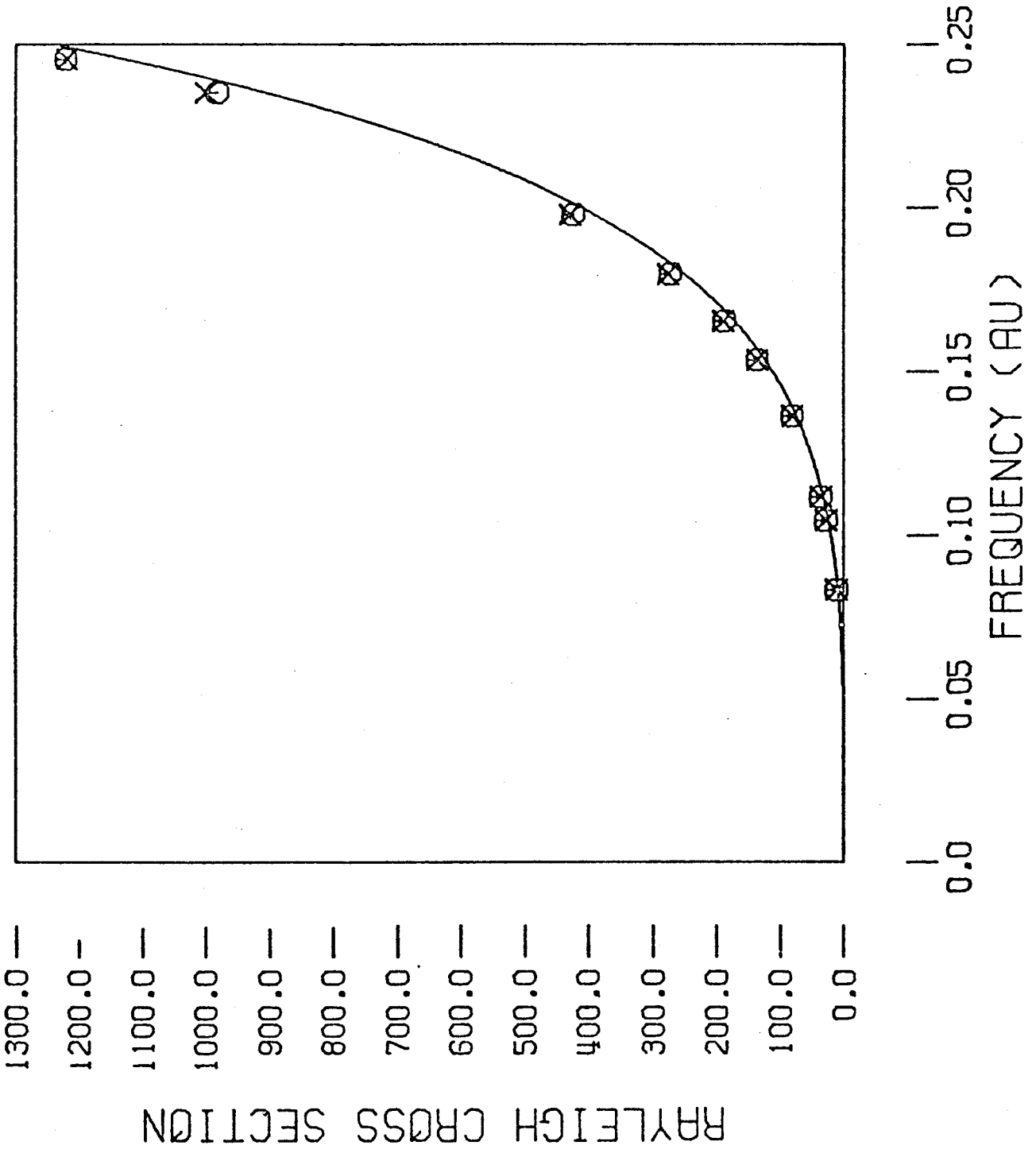
RAYLEIGH CROSS SECTION
1300.0
1200.0
1100.0
1000.0
900.0
800.0
700.0
600.0
500.0
400.0
300.0
200.0
100.0
0.0
0.0
0.05
0.10
0.15
0.20
0.25
FREQUENCY (AU)

Figure 8.

Part II - Photoionization Cross Sections for H_2 in the Random Phase Approximation with a Square-Integrable Basis

1. Introduction

Although experimental photoionization cross sections have been measured for many molecules [1], there have been very few accurate calculations of these cross sections. The major difficulties are in the calculation of accurate molecular continuum wavefunctions and in the sensitivity of these cross sections to the approximations used in calculating the wavefunctions [2, 3]. In particular, electron correlation has been known to have a significant effect on the calculated photoionization cross sections.

Unlike the previous calculations of molecular photoionization cross sections we completely obviate the need for continuum functions, thus resolving the major difficulty in such calculations. The central idea is to obtain a discrete representation of the frequency-dependent polarizability which, although not physical at energies in the continuum, often provides an adequate representation of the polarizability for complex values of the energy. Numerical analytic continuation can then be used to return to the real energy axis where the physical information is desired. The application of this L^2 method to the calculation of photoionization cross sections was suggested by Broad and Reinhardt [4] who applied it to atomic hydrogen. Rescigno, McCurdy, and McKoy [5] have recently used the same method to obtain cross sections for He. The calculated cross sections agreed well with experiment. There [5] a discrete representation of the frequency-dependent polarizability in the random phase approximation (RPA) was used. In this paper we apply the same procedure to molecular hydrogen. The method is applicable to larger molecules since L^2-RPA calculations can be routinely carried out for these systems, e.g., H_2CO, C_2H_4, CO_2, and C_6H_6 [6].

In the following section we briefly review the continuation method and the RPA. In Section 3 we discuss our results and their comparison with experiment.

2. Theory

The frequency-dependent polarizability of an atom or molecule is given by

$$\alpha(z) = \sum_{n\neq o} \frac{f_{on}}{\omega_{on}^2 - z^2} + \int_{\epsilon_I}^{\infty} \frac{g(\epsilon)d\epsilon}{\epsilon^2 - z^2} \quad , \tag{1}$$

where ω_{on}, f_{on}, and $g(\epsilon)$ are the transition frequencies and the bound and continuum oscillator strengths, respectively, and ϵ_I is the first ionization threshold of the system. In the limit $z \rightarrow \omega + i\eta$, eq.(1) yields

$$\alpha(\omega) = \sum_{n\neq o} \frac{f_{on}}{\omega_{on}^2 - \omega^2} + P\int_{\epsilon_I}^{\infty} \frac{g(\epsilon)d\epsilon}{\epsilon^2 - \omega^2} + \frac{i\pi g(\omega)}{2\omega} \tag{2}$$

and thus we have the relation between the photoionization cross section and the imaginary part of $\alpha(\omega)$

$$\sigma(\omega) = \lim_{\eta \rightarrow o} \frac{4\pi\omega}{c} \mathrm{Im}[\alpha(\omega + i\eta)] \quad . \tag{3}$$

To use eq.(3), $\alpha(z)$ is first approximated by a finite sum

$$\alpha(z) \approx \sum_{n} \frac{f_{on}}{\omega_{on}^2 - z^2} \quad . \tag{4}$$

To continue $\alpha(z)$ of eq.(4) analytically on to the real axis, we construct a low-order rational-fraction representation of $\alpha(z)$ by fitting it to the approximate $\alpha(z)$ of eq.(4) at a number of points in the complex plane. We use the algorithm given by Schlessinger et al.[6] to perform this point-wise fitting. We thus obtain a smooth representation of $\alpha(z)$ and can now evaluate $\alpha(\omega)$, and hence $\sigma(\omega)$, at real energies where the original discrete approximation is unphysical.

In the present work the finite set of oscillator strengths and transition frequencies needed to obtain the discrete representation of $\alpha(z)$, eq.(4), is generated by solving the equations of motion in the low-order single particle-hole (1p-1h) pair approximation, the usual random phase approximation. The equations of motion method has been discussed previously [7]. It can be shown that if the state $|n\rangle$ is single particle-hole excited relative to the ground state $|o\rangle$ the equation of motion for the excitation energy ω_{on} and elements of the transition density Y(n) and Z(n) become

$$\begin{pmatrix} \underset{\sim}{A} & \underset{\sim}{B} \\ -\underset{\sim}{B}^* & -A^* \end{pmatrix} \begin{pmatrix} Y(n) \\ Z(n) \end{pmatrix} = \omega_{on} \begin{pmatrix} \underset{\sim}{D} & o \\ o & \underset{\sim}{D} \end{pmatrix} \begin{pmatrix} Y(n) \\ Z(n) \end{pmatrix} . \qquad (5)$$

The matrices $\underset{\sim}{A}$, $\underset{\sim}{B}$, and $\underset{\sim}{D}$ are ground state expectation values of second-quantized operators [7]. If $|o\rangle$ is taken to be the Hartree-Fock ground state, $\underset{\sim}{D}$ becomes the unit matrix and the familiar RPA equations result [7]. The oscillator strengths f_{on} are obtained directly from the ω_{on}'s and the $\{Y(n)\}$ and $\{Z(n)\}$ vectors.

The RPA is a particularly convenient method for constructing the discrete representation of the frequency-dependent polarizability. The dipole length and velocity expressions for the oscillator strength are equivalent in this approximation and the f-sum rule is satisfied [8].

3. Results

The RPA equations for H_2 were solved in a discrete Gaussian basis. The resulting spectrum consists of fourteen $X\ ^1\Sigma_g^+ \rightarrow\ ^1\Sigma_u^+$ transitions and seven $X\ ^1\Sigma_g^+ \rightarrow\ ^1\Pi_{ux}$ transitions. Hence the parallel and perpendicular components of $\alpha(z)$, eq. (4), contain fourteen and seven poles, respectively. The calculations were done at the ground state equilibrium geometry of R = 1.4 a.u. The results of these calculations have been reported elsewhere [9, 10] where they were used to calculate the second-order optical properties and van der Waals coefficients in good agreement with experimental data as well as with other theoretical estimates. Of particular importance for the present purposes is that the resulting oscillator strength distribution satisfied the Thomas-Reiche-Kuhn sum rule exactly and several other energy-weighted sum rules approximately [9, 10]. Moreover, the transition moments for the $X\ ^1\Sigma_g^+ \rightarrow B\ ^1\Sigma_u^+$ and $X\ ^1\Sigma_g^+ \rightarrow C\ ^1\Pi_u$ transitions agree very well with those of the extensive calculations of Wolniewicz [11].

By analytical continuation of the parallel and perpendicular components of $\alpha(z)$ we can obtain the photoionization cross sections for the $^1\Sigma_u^+$ and $^1\Pi_u$ channels separately. Since there is no a priori rule for determining the fitting points for determining the rational-fraction representation of eq. (4), we obtained the photoionization cross sections for several choices of fitting points. These points were chosen with a real part between each pair of frequencies and the imaginary parts were varied over a wide region of the complex plane. Figures 1 and 2 show the $\sigma(\Sigma_u^+)$ and $\sigma(\Pi_u)$ photoionization cross sections obtained by continuation of rational fractions with three different choices of fitting points. At photon frequencies near threshold, i.e., the vertical ionization potential of 16.4 eV for H_2, the calculated cross sections are within 5-10% of one another for the different choices of the fitting points. At frequencies away from threshold,

the calculated cross sections are insensitive to the choice of fitting points for the analytic continuation.

In Table I and fig. 3 we compare the total calculated photoionization cross sections for H_2 with the experimental results of Cook and Metzger [12], Samson and Cairns [13], and Rebbert and Ausloos [14]. The calculated cross sections are those for the vertical photoionization of H_2 and hence the threshold is at 16.4 eV. The $v' = 0$, $v'' = 0$ ionization threshold for H_2 is about 15.5 eV. Our calculated cross sections should be compared with the experimental ones only at frequencies above those for which the sum of all Franck-Condon factors for the open vibrational channels of H_2^+ are close to unity. From the Franck-Condon factors for the $H_2 - H_2^+$ system, this begins at photon energies around 18 eV. In a future publication [15] we plan to include these Franck-Condon factors and the effect of the variation of internuclear distance on the electronic polarizability.

From Table I and fig. 3 we see that our calculated cross sections agree well with the measured cross sections. These cross sections are closer to the experimental cross sections than those of Kelly [16] who used molecular continuum eigenfunctions and neglected electron correlation.

4. Conclusions

These results for the photoionization cross sections of H_2 again indicate that it is not necessary to employ continuum basis functions in molecular photoionization calculations. Moreover, the calculations on larger molecules by this method require only modest additional computational effort. Calculations on the photoionization cross sections of N_2, H_2CO, CO_2, and C_6H_6 are underway. Finally, since we obtain the photoionization cross sections into separate symmetry channels we can obtain angular distribution for H_2 since phase shifts are available or can be calculated.

5. Acknowledgements

The authors thank Dr. G. R. Cook for kindly supplying detailed information on his experimental photoionization cross sections. One of us (VM) thanks Dr. Carl Moser of CECAM (Paris) for his hospitality and support during his recent visit there. PHSM thanks the Conselho Nacional de Pesquisas (Brasil) for financial support and the Universidade Federal do Rio de Janeiro for a leave of absence. He (PHSM) is also grateful to Anna Martin for help in the preparation of the manuscript.

Table 1

Comparison of calculated photoionization cross sections with the observed cross sections at selected wavelengths.

Wavelength (Å)	Photon Energy (eV)	Calculated [a] cross sections (Mb)	Experimental cross sections (Mb)
741	16.7	10.74	9.18[b]
			10.48[c]
713	17.4	9.95	10.15[d]
685	18.1	9.25	9.85
675	18.4	9.03	9.63
661	18.8	8.69	9.00
646	19.2	8.36	8.63
620	20.0	7.82	7.70
600	20.7	7.36	6.95
584	21.2	6.98	6.88[e]
452	27.4	3.50	3.37[f]
428	29.0	2.94	2.88
374	33.1	1.86	2.04
359	34.6	1.61	1.75
335	37.0	1.27	1.36
315	39.4	1.02	1.12
298	41.6	0.84	0.95
266	46.6	0.57	0.64
247	50.2	0.45	0.49
234	52.9	0.37	0.40

Table 1 (continued)

---

[a] In megabarns or 10^{-18} cm^2.

[b] Reference 12.

[c] Reference 14. This is the cross-section in the 736-744 Å range.

[d] The following values are taken from ref. 12.

[e] Reference 14.

[f] The following values are taken from ref. 13.

References

[1] R. D. Hudson, Natl. Std. Ref. Data Ser., Natl. Bur. Stds. (U.S.) 38 (1971).

[2] G. V. Marr, Photoionization Processes in Gases (Academic Press, New York, 1967).

[3] M. Ya. Amusia, N. A. Cherepkov, and L. V. Chernysheva, Soviet Phys. JETP 33 (1971) 90.

[4] J. Broad and W. P. Reinhardt, J. Chem. Phys. 60 (1974) 2182.

[5] T. N. Rescigno, C. W. McCurdy, Jr., and V. McKoy, Phys. Rev. A (June, 1974).

[6] H_2CO: D. L. Yeager and V. McKoy, J. Chem. Phys. 60 (1974) 2714; C_2H_4: J. Rose, T. Shibuya, and V. McKoy, J. Chem. Phys. 58 (1973) 74; C_6H_6: J. Rose, T. Shibuya, and V. McKoy, J. Chem. Phys. 60 (1974) 2700; CO_2: C. W. McCurdy and V. McKoy, J. Chem. Phys. (December 1, 1974).

[7] T. Shibuya and V. McKoy, Phys. Rev. A 2 (1970) 2208.

[8] R. A. Harris, J. Chem. Phys. 50 (1969) 3947; D. J. Rowe, Nuclear Collective Motion (Methuen, London, 1970), p. 274.

[9] P. H. S. Martin, W. H. Henneker, and V. McKoy, Chem. Phys. Letters (accepted for publication).

[10] P. H. S. Martin, W. H. Henneker, and V. McKoy, J. Chem. Phys. (accepted for publication).

[11] L. Wolniewicz, J. Chem. Phys. 51 (1969) 5002.

[12] G. R. Cook and P. H. Metzger, J. Opt. Soc. Am. 54 (1964) 968.

[13] J. A. R. Samson and R. B. Cairns, J. Opt. Soc. Am. 55 (1965) 1035.

[14] R. E. Rebbert and P. Ausloos, J. Res. Natl. Bur. Std. A.Phys. and Chem. 75A (1971) 481.

[15] P. H. S. Martin, W. H. Henneker, and V. McKoy, J. Chem. Phys. (to be published).

[16] H. P. Kelly, Chem. Phys. Letters 20 (1973) 547.

Figure Captions

Figure 1. Photoionization cross section of H_2 for the $X^1\Sigma_g^+ \rightarrow {}^1\Sigma_u^+$ channel. The curves show the results for three different choices of fitting points used for constructing the rational fraction. Cross sections are in units of megabarns.

Figure 2. Photoionization cross section of H_2 for the $X\,{}^1\Sigma_g^+ \rightarrow {}^1\Pi_u$ channel. The curves show the results for three different choices of fitting points used for constructing the rational fraction. Cross sections are in units of megabarns.

Figure 3. Comparison of calculated total photoionization cross sections with experimental data. The points are taken from references 12 and 13. See footnotes in Table 1.

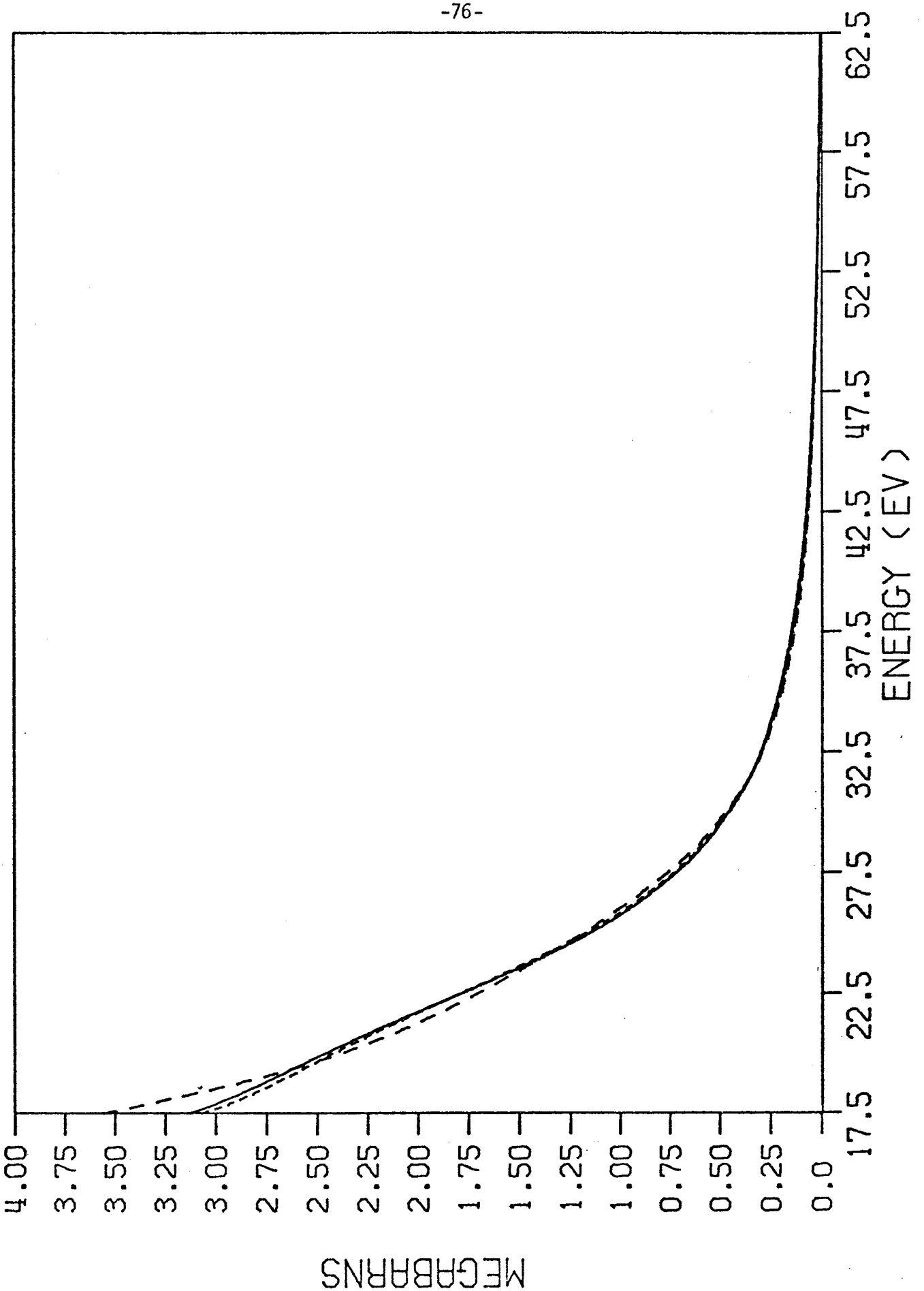
MEGABARNS
4.00
3.75
3.50
3.25
3.00
2.75
2.50
2.25
2.00
1.75
1.50
1.25
1.00
0.75
0.50
0.25
0.0
17.5
22.5
27.5
32.5
37.5
42.5
47.5
52.5
57.5
62.5
ENERGY (EV)

Figure 1.

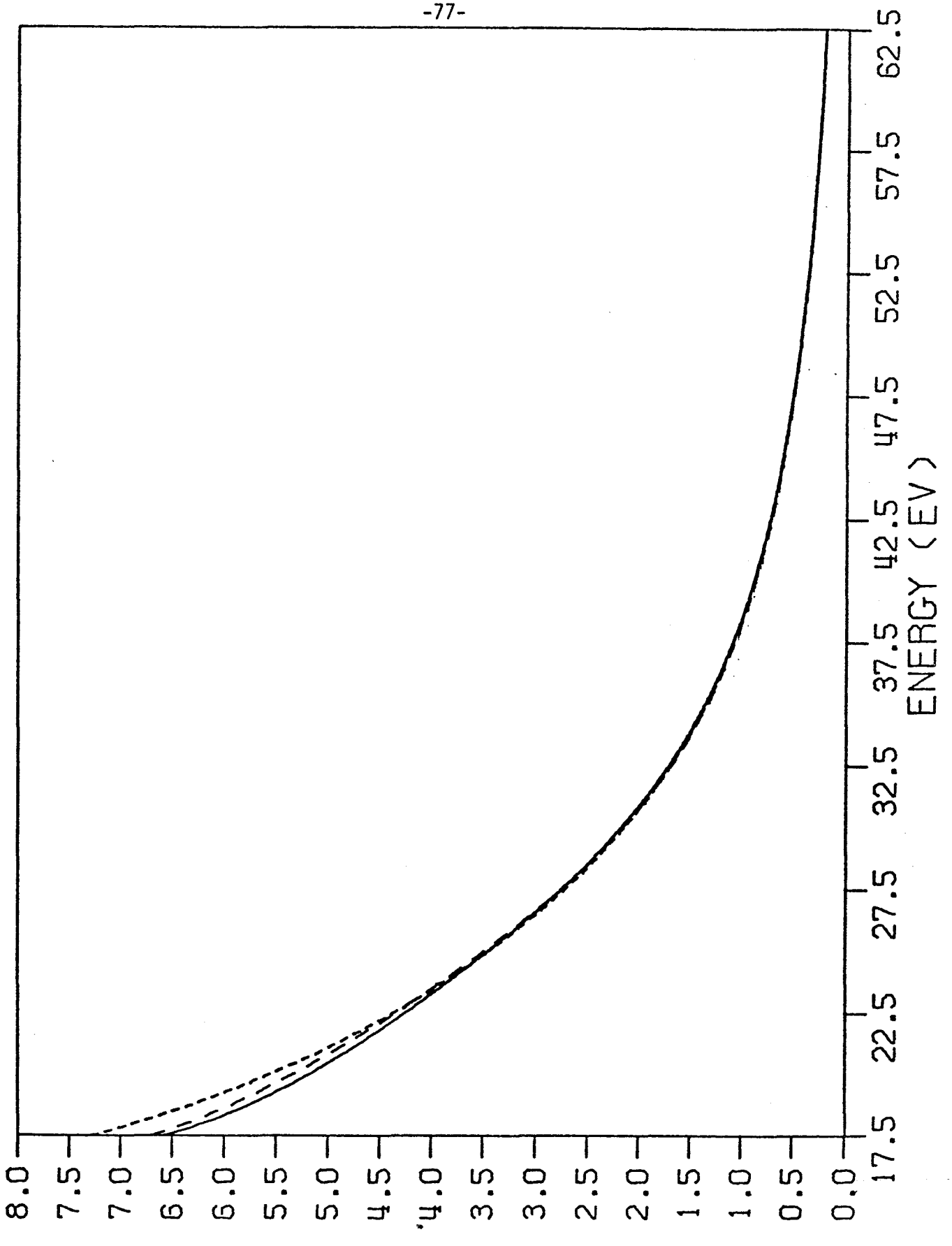
MEGABARNS
8.0
7.5
7.0
6.5
6.0
5.5
5.0
4.5
4.0
3.5
3.0
2.5
2.0
1.5
1.0
0.5
0.0
17.5
22.5
27.5
32.5
37.5
42.5
47.5
52.5
57.5
62.5
ENERGY (EV)

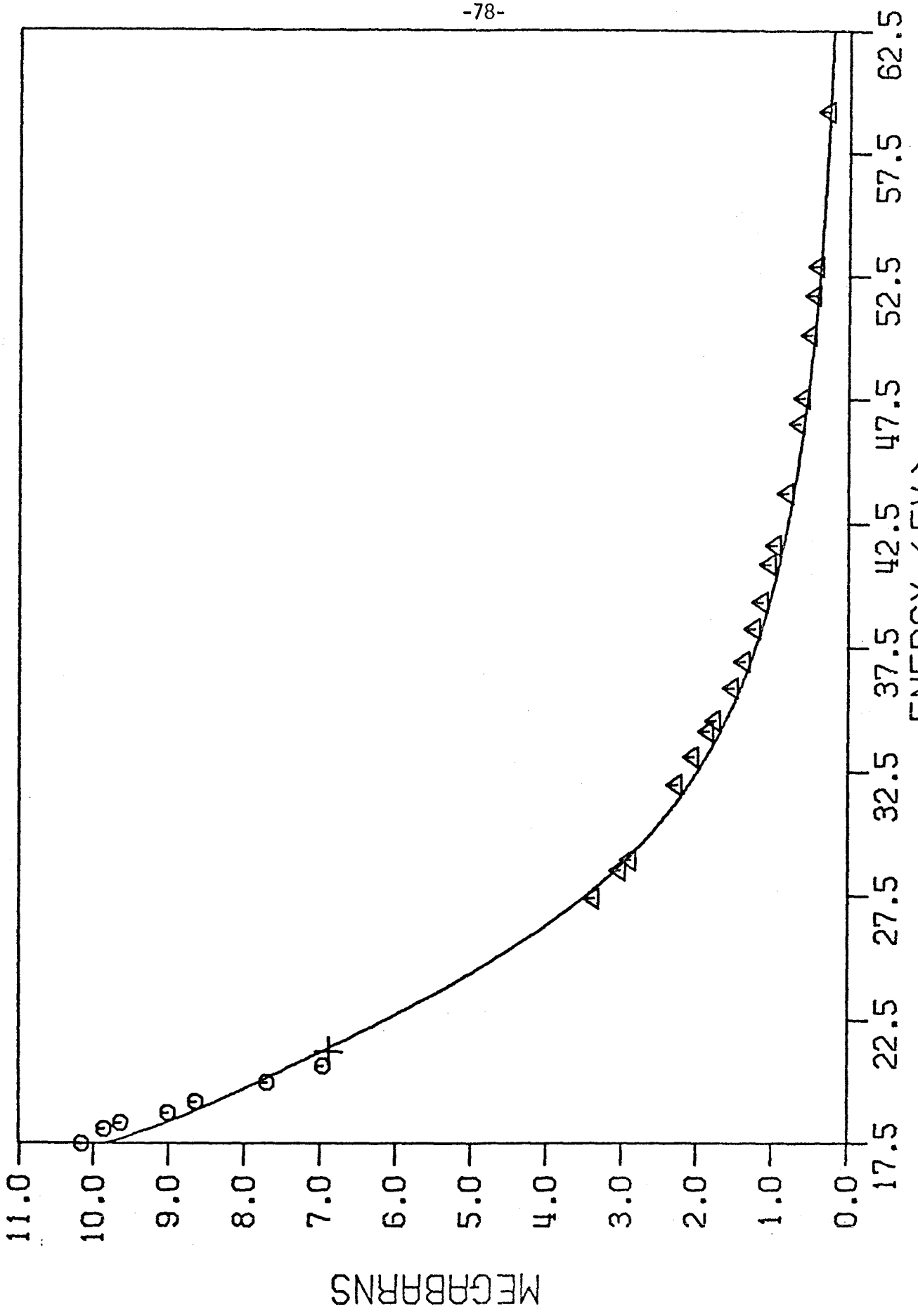
MEGABARNS
11.0
10.0
9.0
8.0
7.0
6.0
5.0
4.0
3.0
2.0
1.0
0.0
17.5
22.5
27.5
32.5
37.5
42.5
47.5
52.5
57.5
62.5
ENERGY (EV)

Figure 3.

Part III - Oscillator Strengths for the $X^1\Sigma^+ - A^1\Pi$ System in CH^+ from the Equations of Motion Method

1. INTRODUCTION

With the recent expansion of the field of astrochemistry and studies of the formation and evolution of interstellar clouds, the need has arisen for accurate and reliable molecular data[1] on species not previously investigated in any detail either experimentally or theoretically. A thorough discussion of current astrophysical and astrochemical problems related to molecule formation in interstellar space can be found in Ref. 2.

A typical example of a situation where the lack of reliable molecular data has seriously affected the development of models for the formation of interstellar molecules is that of the relative abundances of CH and CH^+ and their formation through radiative association processes from atoms and ions.[3] In particular, the rate of association of C and H^+ to form CH^+ depends on the oscillator strength of the $X^1\Sigma^+ - A^1\Pi$ transition in CH^+.[3-5] CH^+ is charged and a highly reactive species, which makes spectroscopic studies in the laboratory difficult. Under these circumstances, detailed theoretical calculations become appealing. One of the early theories[6] of the formation of CH^+ was initially discarded because the assumed f-values lead to low rates of radiative association. However, the work of Solomon and Klemperer[3] revived the interest in this radiative association mechanism by reevaluating the rates by using better f-values.

In addition to these direct processes Julienne and Krauss[4] have discussed an alternative mechanism, namely, indirect radiative association (inverse predissociation) leading to the formation of other species as well, such as NO, CH, CO, C_2, etc. In these studies a reliable source of

intensities is necessary if we are to reduce the uncertainties in models of the interstellar medium.

For these reasons, considerable effort has been put into the ab initio quantum mechanical calculation of the potential energy curves[7] and oscillator strengths[8] of CH^+. Similar work has been done on CH[9].

In this paper we present the oscillator strength of the $X^1\Sigma^+ - A^1\Pi$ transition of CH^+ as computed by the Equations of Motion Method.[10] Our result is in good agreement with the extensive CI calculations of Green et al.,[7] and Yoshimine et al.[8] The results presented are important because they constitute an independent confirmation of the results of Green et al., and Yoshimine et.al., using a different approach. Moreover, computationally the method is simple and relatively inexpensive. This is an important feature since the rapidly expanding fields of astrophysics and astrochemistry of the interstellar medium require reliable estimates of molecular parameters such as excitation energies and transition moments at various geometries. Since it is not always possible to study the systems of interest experimentally, we must resort to theoretical calculations that, while still reliable, do not represent a major computational effort.

2. THEORY AND RESULTS

The Equations of Motion (EOM) Method for calculating excitation energies and transition moments has been thoroughly described elsewhere[10] and here we only outline some of the central ideas.

In this approach we define an excitation operator such that

$$O_\lambda^+ |O\rangle = |\lambda\rangle \tag{1}$$

where $|\lambda\rangle$ is some excited state and $|0\rangle$ is the ground state. It then can be shown that O_λ^+ satisfies an equation of motion[11] given by

$$\langle O | [\delta O_\lambda, H, O_\lambda^+] | O\rangle = \omega_\lambda \langle O | [\delta O_\lambda, O_\lambda^+] | O\rangle \tag{2}$$

where the double commutator is defined by

$$2[A,B,C] = [[A,B],C] + [A,[B,C]] \tag{3}$$

ω_λ is the excitation frequency and δO_λ^+ represents a variation of the amplitudes specifying O_λ^+. If O_λ^+ is assumed to be composed of single particle-hole pairs (1p-1h) the equations of motion become

$$\begin{bmatrix} \underset{\sim}{A} & \underset{\sim}{B} \\ -\underset{\sim}{B}^* & -\underset{\sim}{A}^* \end{bmatrix} \begin{bmatrix} \underset{\sim}{Y}(\lambda) \\ \underset{\sim}{Z}(\lambda) \end{bmatrix} = \omega_\lambda \begin{bmatrix} \underset{\sim}{D} & O \\ O & \underset{\sim}{D} \end{bmatrix} \begin{bmatrix} \underset{\sim}{Y}(\lambda) \\ \underset{\sim}{Z}(\lambda) \end{bmatrix} \tag{4}$$

The elements of the matrices $\underset{\sim}{A}$, $\underset{\sim}{B}$, and $\underset{\sim}{D}$, are given in Ref. 10. $\underset{\sim}{Y}$ and $\underset{\sim}{Z}$ are the amplitudes we wish to calculate. Higher order approximations (inclusion of 2p-2h components) to the exact Eq. 2 can also be easily constructed. In the above approach we obtain spectroscopic quantities of interest e.g. transition intensities directly, and avoid the calculation of

of highly accurate and elaborate total wavefunctions and absolute energies for the different electronic states separately.

In this paper we report calculations on CH^+ using two different gaussian basis sets: a [3S2P/2S] contracted from a (9S5P/4S)[12a] primitive basis and a more recent version of the [3S2P/2S] contraction[12b] to which we added polarization functions. The final basis was then [3S2P1D/2S1P].

In Table I we summarize the results we obtain with the two bases and compare them with the best CI calculations to date.[7,8] We have performed the calculation only at one internuclear distance, namely 1.12 Å, which is the ground state equilibrium geometry. The first column in the table, labeled RPA (Random Phase Approximation) is derived from lowest order single particle-hole pair (1p-1h) solutions to the equations of motion. (See Ref. 10). The column labeled EOM, contains results that were not fully iterated.[10] Continuing the iterations may have improved the excitation energy somewhat within the rather small basis set being used. The basis was chosen to provide good results for the $X\ ^1\Sigma^+ - A^1\Pi$ transition moment, since this is the one transition that bears the most astrophysical interest.

The values we have computed are compared with those obtained by interpolating from the data in references 7 and 8. Overall agreement is good. We want to point out that the size of the problem (computational effort) is determined by the number of 1p-1h excitations included in Eq. 4. In our larger basis ([3S2P1D/2S1P]) this amounts only to 12, which means that at most only 12 × 12 matrices must be diagonalized for states of Π symmetry. Another feature of EOM calculations that makes them

particularly practical is that an SCF run is needed only once and on the ground state exclusively. From a single calculation we obtain most of the low-lying states (all of the symmetries allowed by the basis set being used). As in any basis set expansion technique the quality of the final results depends on the nature and the size of the basis used. However, we have found in general that valence basis sets of relatively poor quality still give very good transition moments and excitation energies to states with small diffuse components.

In conclusion, the EOM scheme can provide reliable molecular spectral data such as excitation energies and oscillator strengths in a computationally simple fashion. Applications to other molecules of interest in astrophysics are underway.

3. ACKNOWLEDGEMENTS

One of us (PHSM) thanks C. W. McCurdy for computational assistance during the early stages of this work.

Table 1.

Vertical Excitation Energy and Oscillator Strength for the $X^1\Sigma^+$-$A^1\Pi$ Transition in CH^+

Property	[3S2P/2S] RPA	[3S2P1D/2S1P] EOM	CI of Refs. 7, 8
Excitation Energy(eV)	2.37	2.50	3.32[a]
Transition Moment(au)	0.34	0.31	0.30[a]
Oscillator Strength	0.014	0.011	0.0147[a]

[a] Values interpolated from the data in references 7 and 8.

REFERENCES

[1] D. McNally, Adv. At. Mol. Phys. 6, 1 (1972).

[2] M. A. Gordon, L. E. Snyder (Editors), "Molecules in the Galactic Environment," Wiley, N.Y., (1973).

[3] P. M. Solomon and W. Klemperer, Ap. J. 178, 389 (1972).

[4] P. S. Julienne, and M. Krauss, in "Molecules in the Galactic Environment," M. A. Gordon and L. E. Synder (Editors), page 354, Wiley, N.Y., (1973).

[5] W. H. Smith, H. S. Liszt, and B. L. Lutz, Ap. J. 183, 69, (1973).

[6] D. R. Bates, Monthly Notices of the Royal Astronomical Society, 111, 303 (1951).

[7] S. Green, P. S. Bagus, B. Liu, A. D. McLean, and M. Yoshimine, Phys. Rev. A5, 1614 (1972).

[8] M. Yoshimine, S. Green, and P. Thaddeus, Ap. J. 183, 899 (1973).

[9] For similar ab initio CI calculations on CH see G. C. Lie, and J. Hinze, J. Chem. Phys. 59, 1872 (1973) and G. C. Lie, J. Hinze, and B. Liu, ibid., p. 1887.

[10] (a) T. I. Shibuya and V. McKoy, Phys. Rev. A2, (1970).

(b) J. Rose, T. I. Shibuya, and V. McKoy, J. Chem. Phys. 58, (1973).

[11] D. J. Rowe, "Nuclear Collective Motion," Methuen, London (1970).

[12] (a) For details see T. H. Dunning, J. Chem. Phys. 53, 2823 (1970).

(b) T. H. Dunning, private communication.